US 20140130415A1

(19) **United States**

(12) **Patent Application Publication**

Chan

(10) **Pub. No.: US 2014/0130415 A1**

(43) **Pub. Date: May 15, 2014**

(54) **METHOD AND SYSTEM FOR PRODUCTION OF HYDROGEN AND CARBON MONOXIDE**

(71) Applicant: **The Trustees of Columbia University in the City of New York**, New York, NY (US)

(72) Inventor: **Siu-wai Chan**, Demarest, NJ (US)

(73) Assignee: **The Trustees of Columbia University in the City of New York**, New York, NY (US)

(21) Appl. No.: **14/160,234**

(22) Filed: **Jan. 21, 2014**

Related U.S. Application Data

(63) Continuation-in-part of application No. PCT/US2012/047303, filed on Jul. 19, 2012.

(60) Provisional application No. 61/509,370, filed on Jul. 19, 2011, provisional application No. 61/638,960, filed on Apr. 26, 2012.

Publication Classification

(51) **Int. Cl.**
C10K 3/02 (2006.01)

(52) **U.S. Cl.**
CPC ***C10K 3/026*** (2013.01)
USPC **48/61**; 48/204

(57) **ABSTRACT**

A method for preparing a fuel using oxygen-storing compound nanoparticles is provided, in which the nanoparticles is heated at a first temperature to release an amount of oxygen, thereby producing a reduced oxide compound, and the reduced oxide compound is exposed to a gas at a second temperature to produce the fuel. The gas can include carbon dioxide and water vapor, and the fuel can include carbon monoxide and/or hydrogen. The oxygen-storing compound nanoparticles can be nano ceria or nano ceria doped with one or more metals, such as Cu and/or Zr. A system for carrying out the method is also disclosed.

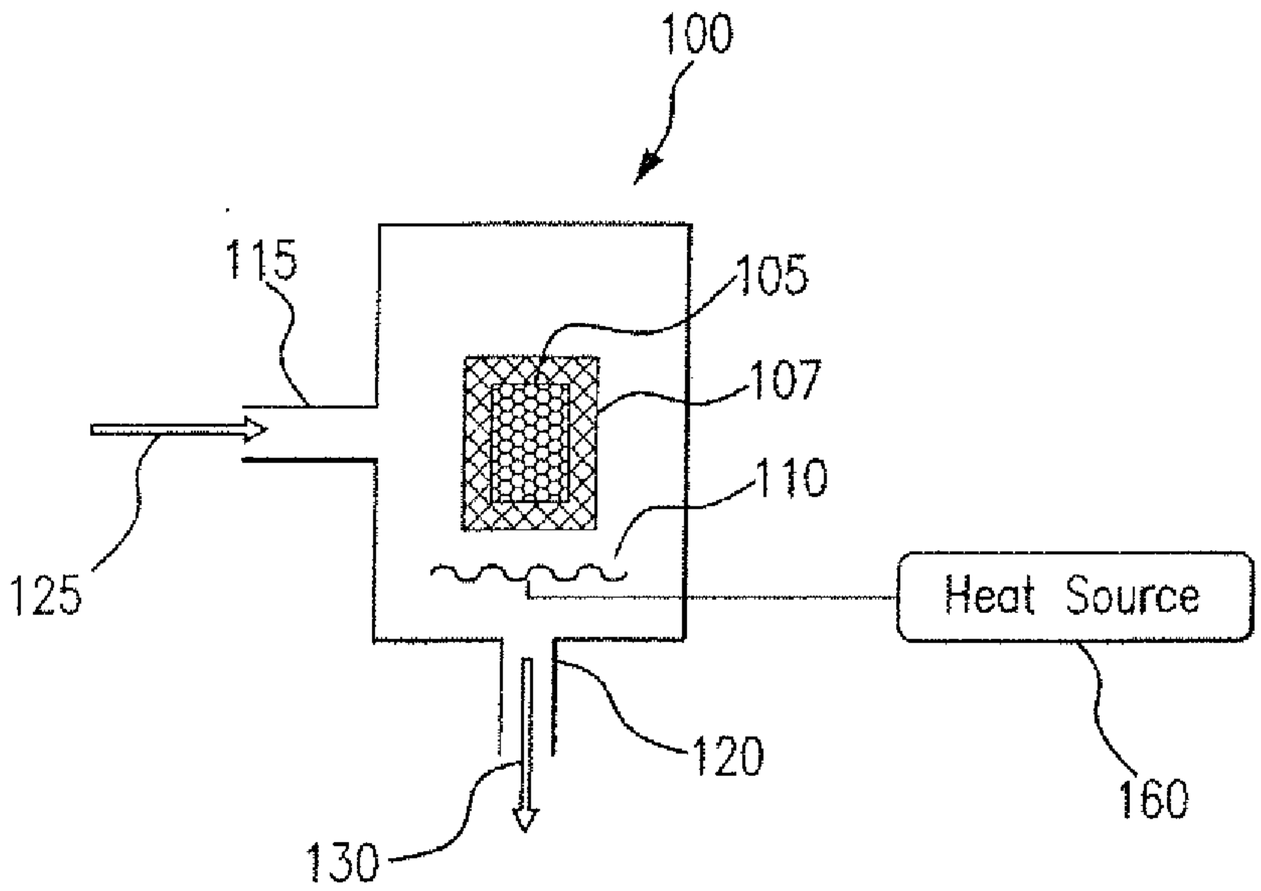

FIG. 1

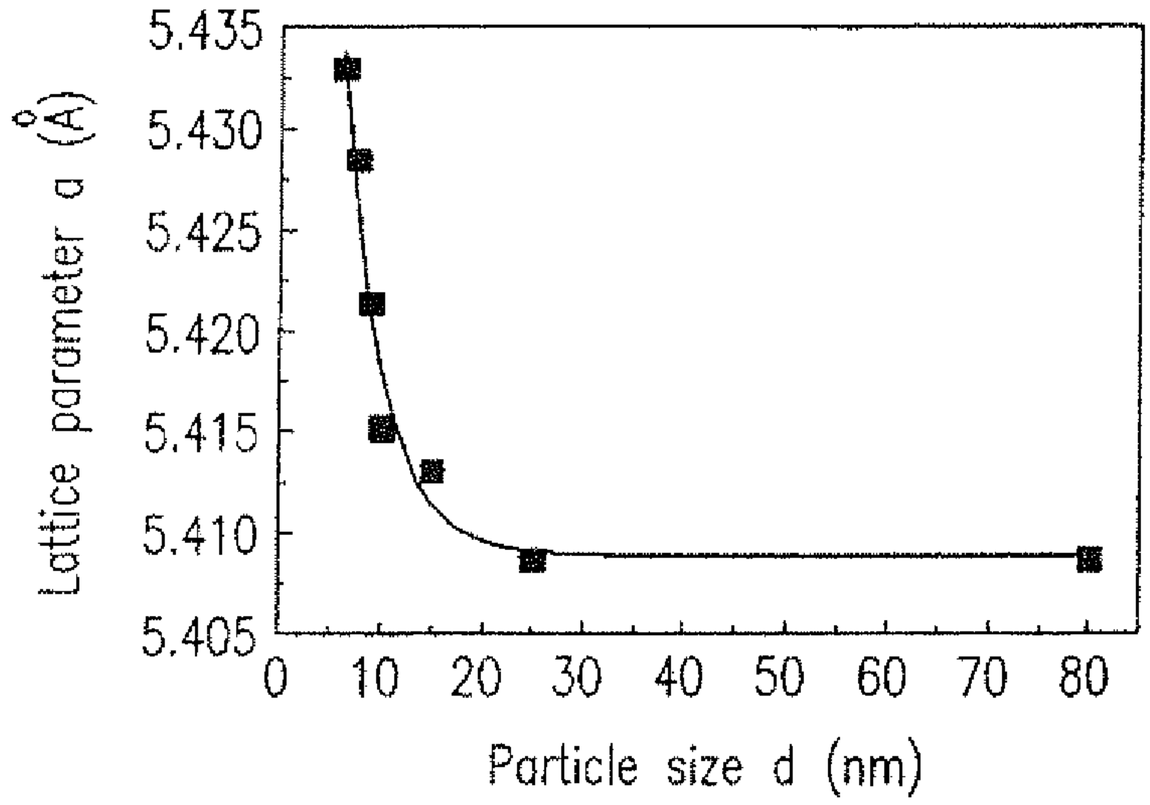
Lattice parameter a (Å)
5.435
5.430
5.425
5.420
5.415
5.410
5.405
0
10
20
30
40
50
60
70
80
Particle size d (nm)

FIG. 2

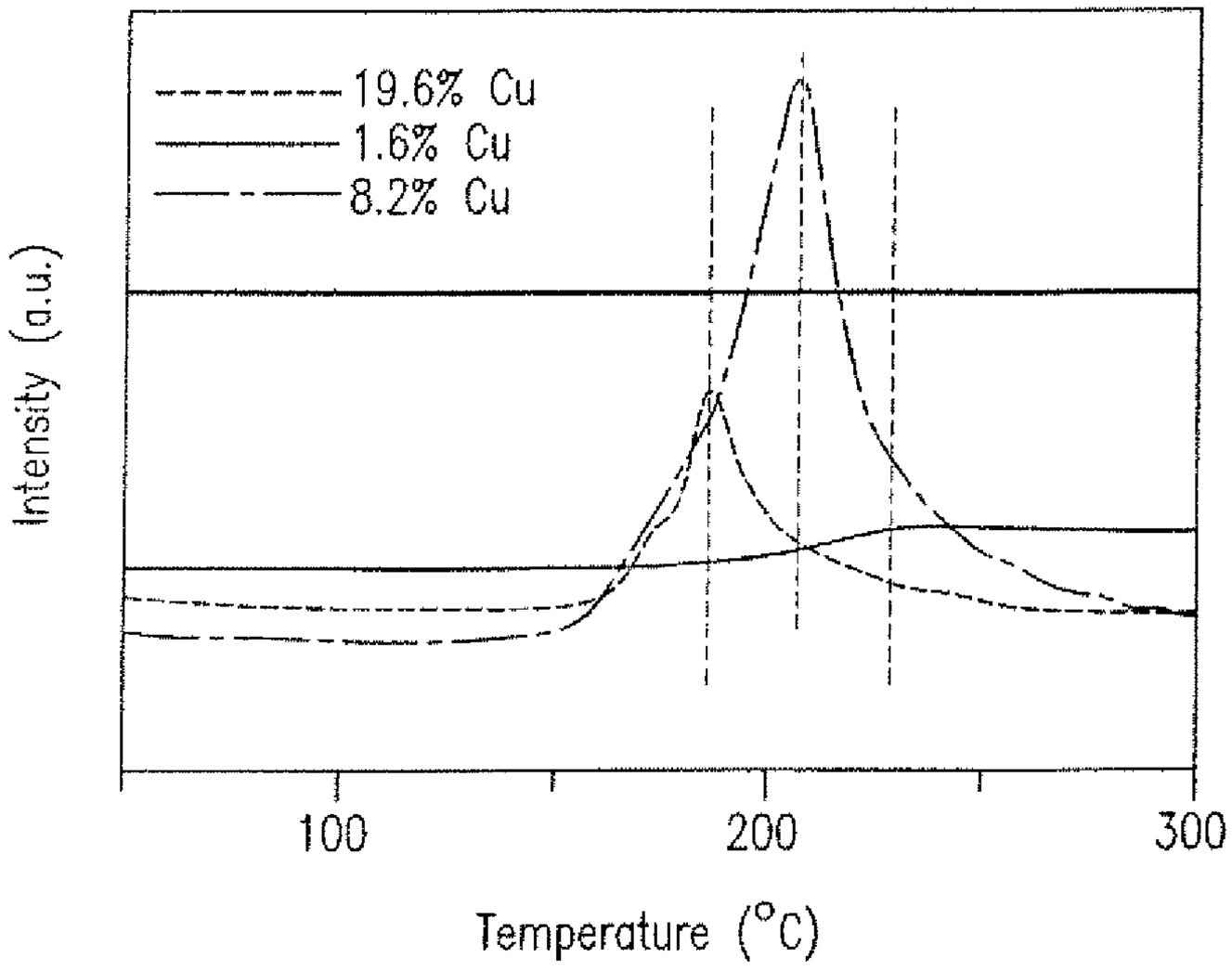

FIG. 3

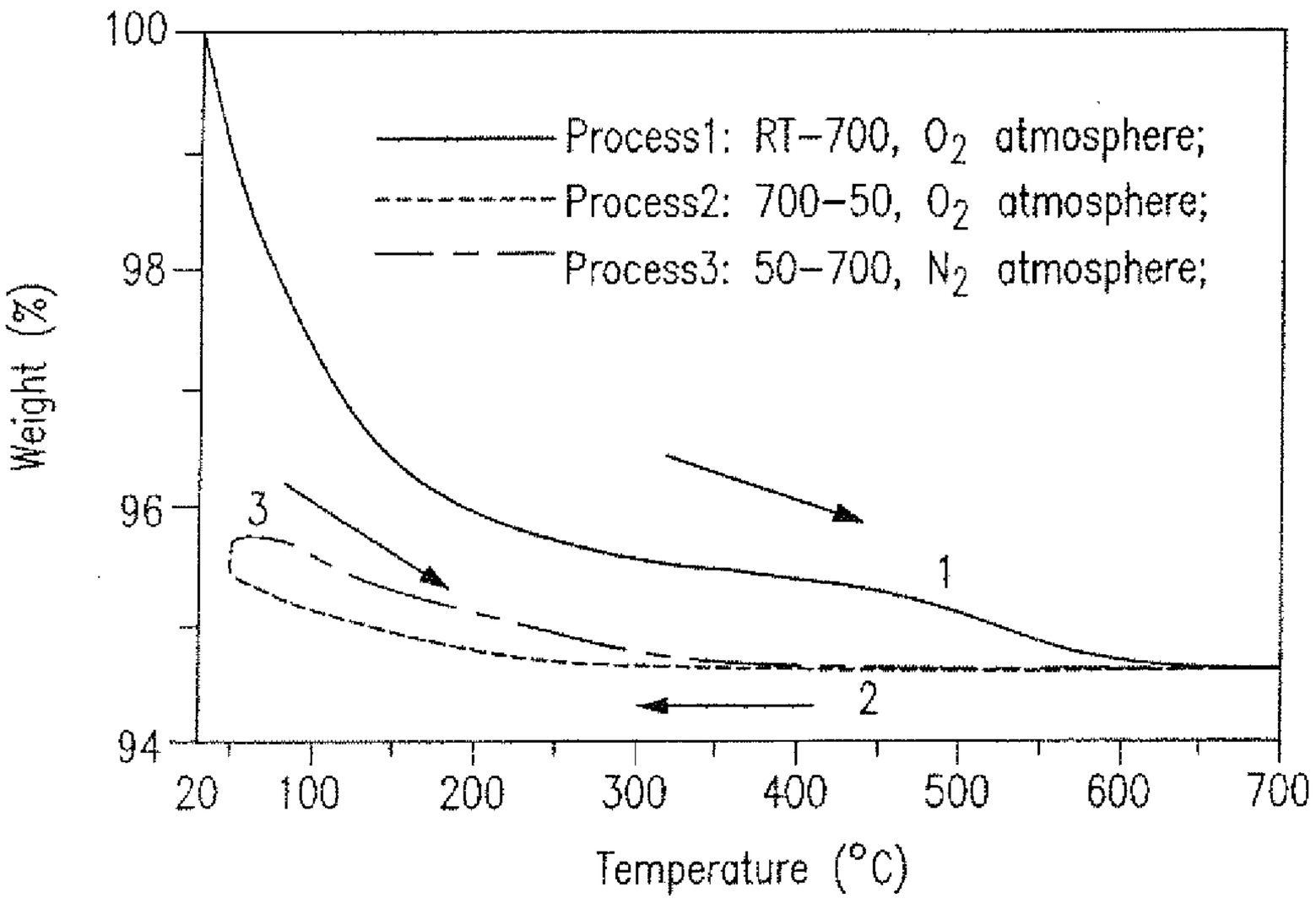
100
98
96
94
Weight (%)
Process1: RT–700, O_2 atmosphere;
Process2: 700–50, O_2 atmosphere;
Process3: 50–700, N_2 atmosphere;
1
2
3
20
100
200
300
400
500
600
700
Temperature (°C)

FIG. 4

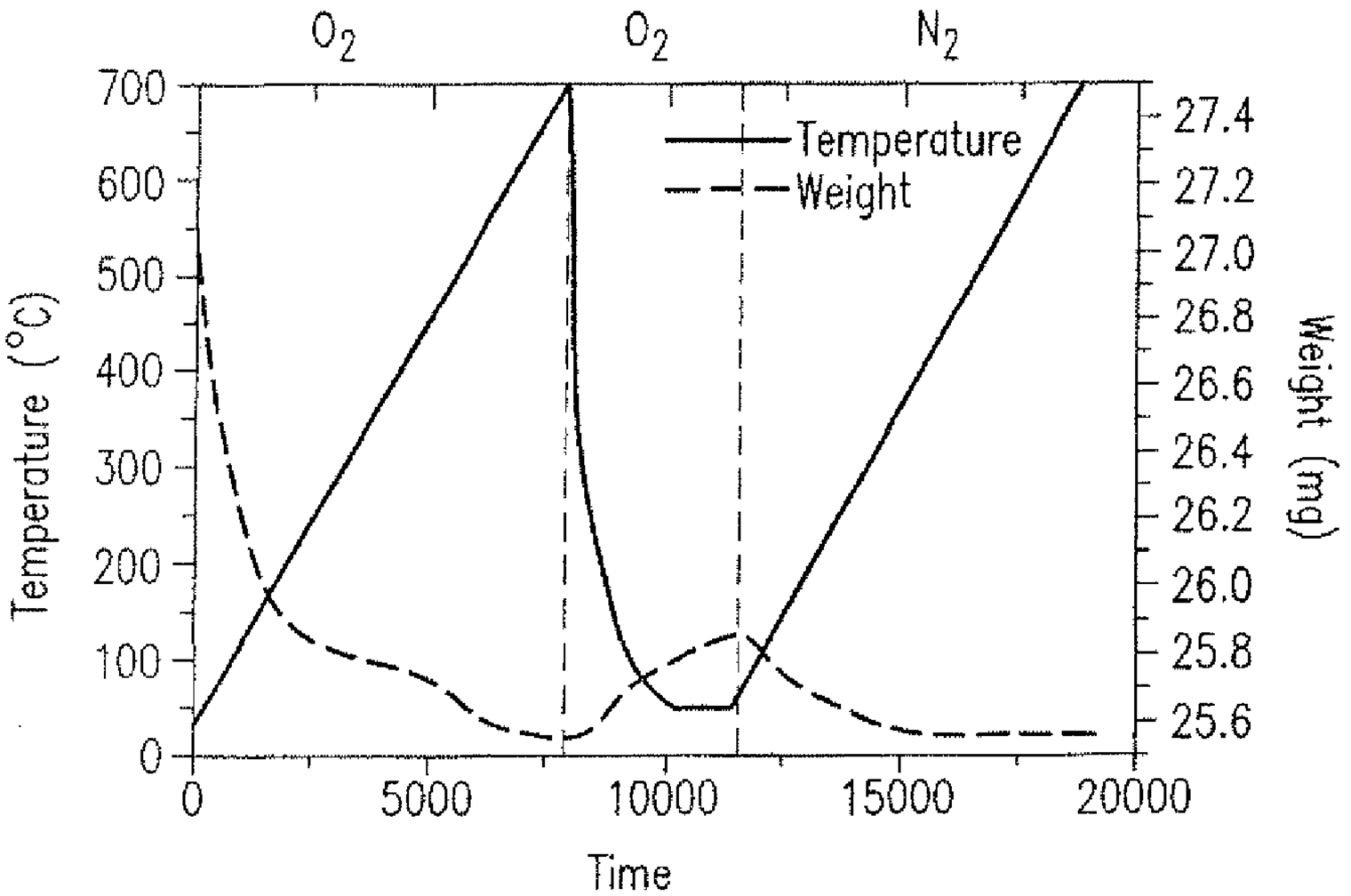
O2
O2
N2
700
600
500
400
300
200
100
0
Temperature (°C)
Temperature
Weight
27.4
27.2
27.0
26.8
26.6
26.4
26.2
26.0
25.8
25.6
Weight (mg)
0
5000
10000
15000
20000
Time

FIG. 5

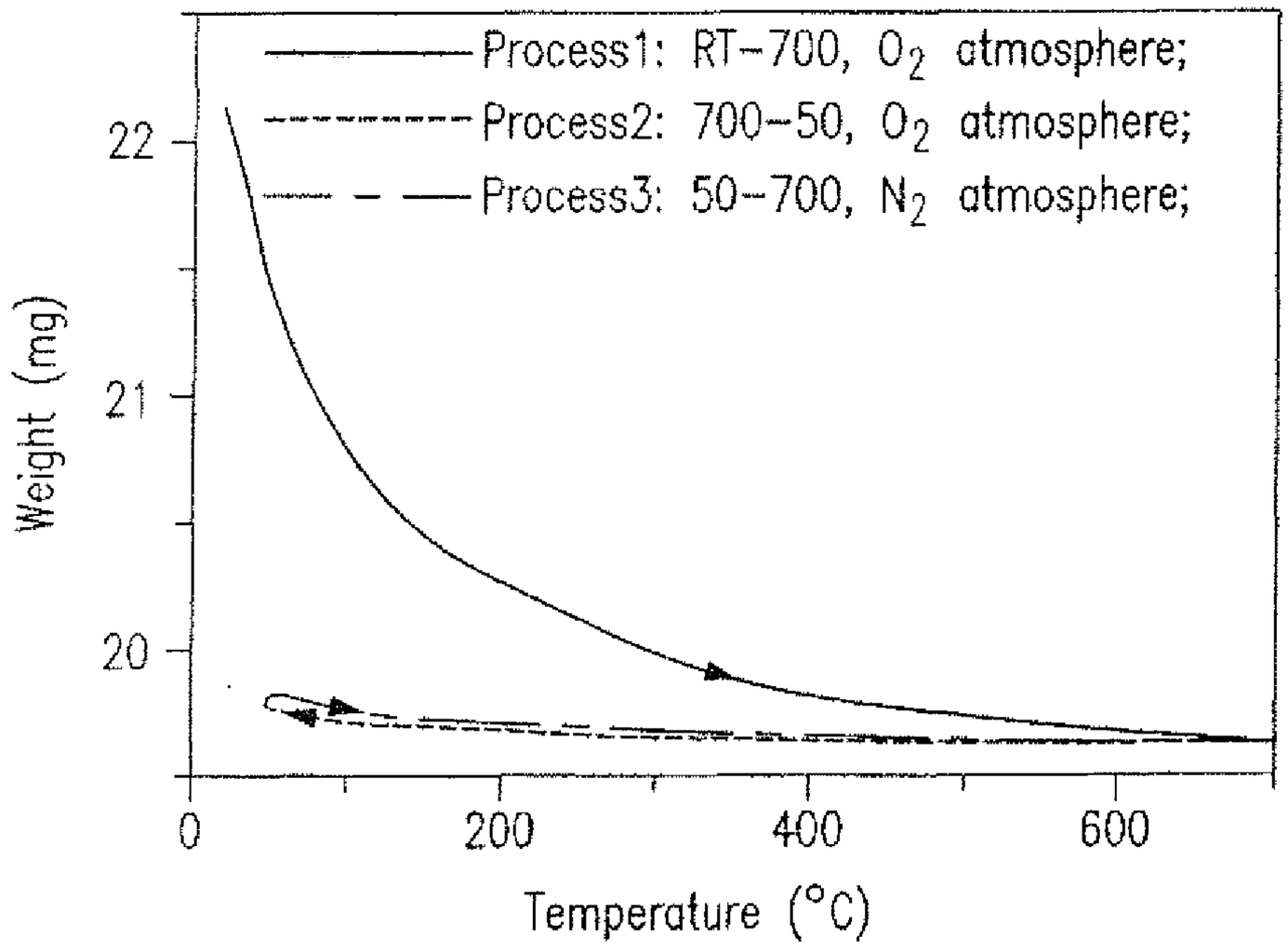
Process1: RT–700, O_2 atmosphere;
Process2: 700–50, O_2 atmosphere;
Process3: 50–700, N_2 atmosphere;
Weight (mg)
22
21
20
0
200
400
600
Temperature (°C)

FIG. 6

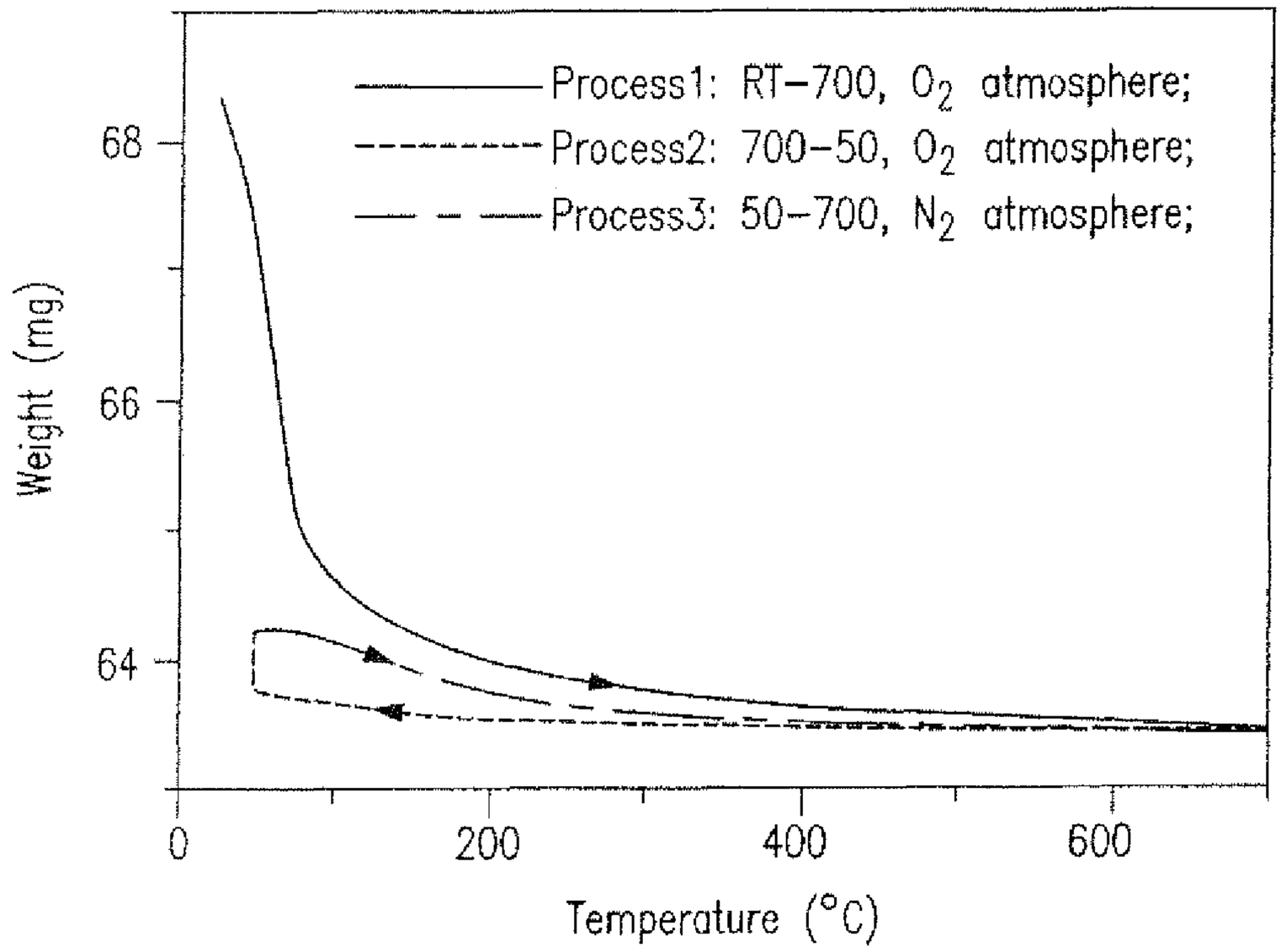
Process1: RT–700, O_2 atmosphere;
Process2: 700–50, O_2 atmosphere;
Process3: 50–700, N_2 atmosphere;
Weight (mg)
68
66
64
0
200
400
600
Temperature (°C)

FIG. 7

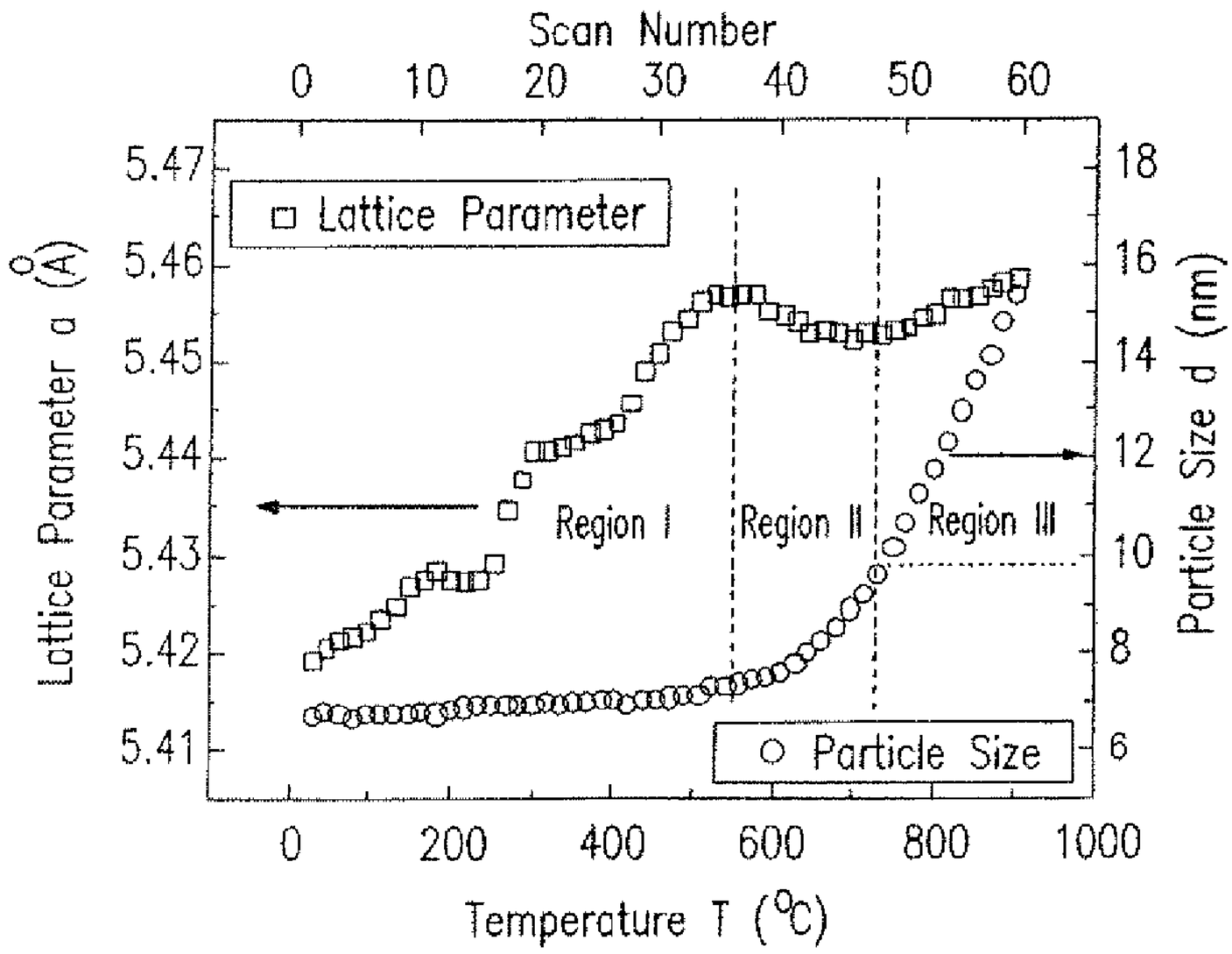
Scan Number
0
10
20
30
40
50
60
Lattice Parameter
Particle Size
Region I
Region II
Region III
Lattice Parameter a (Å)
Particle Size d (nm)
5.47
5.46
5.45
5.44
5.43
5.42
5.41
18
16
14
12
10
8
6
0
200
400
600
800
1000
Temperature T (°C)

FIG. 8

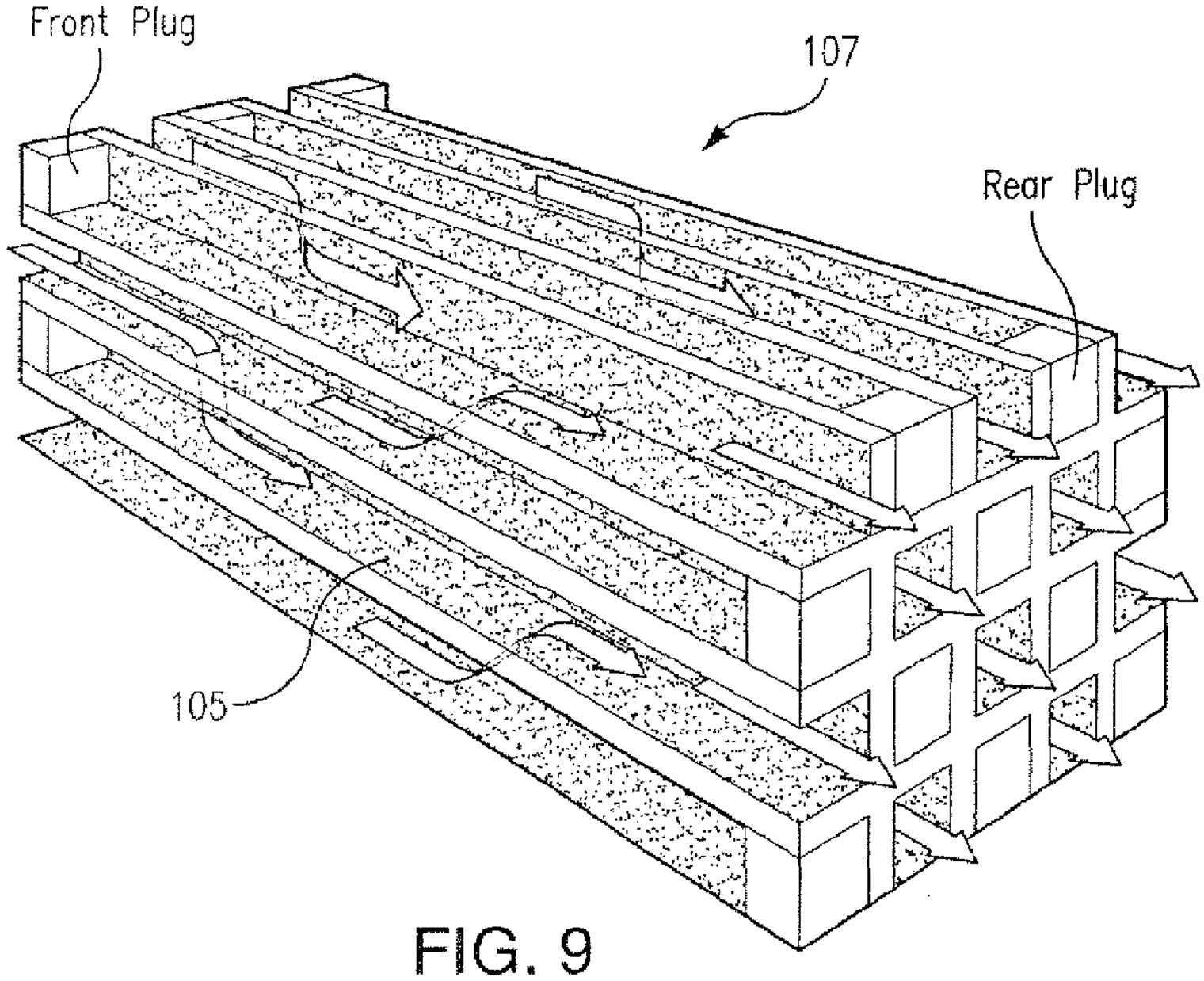

FIG. 9

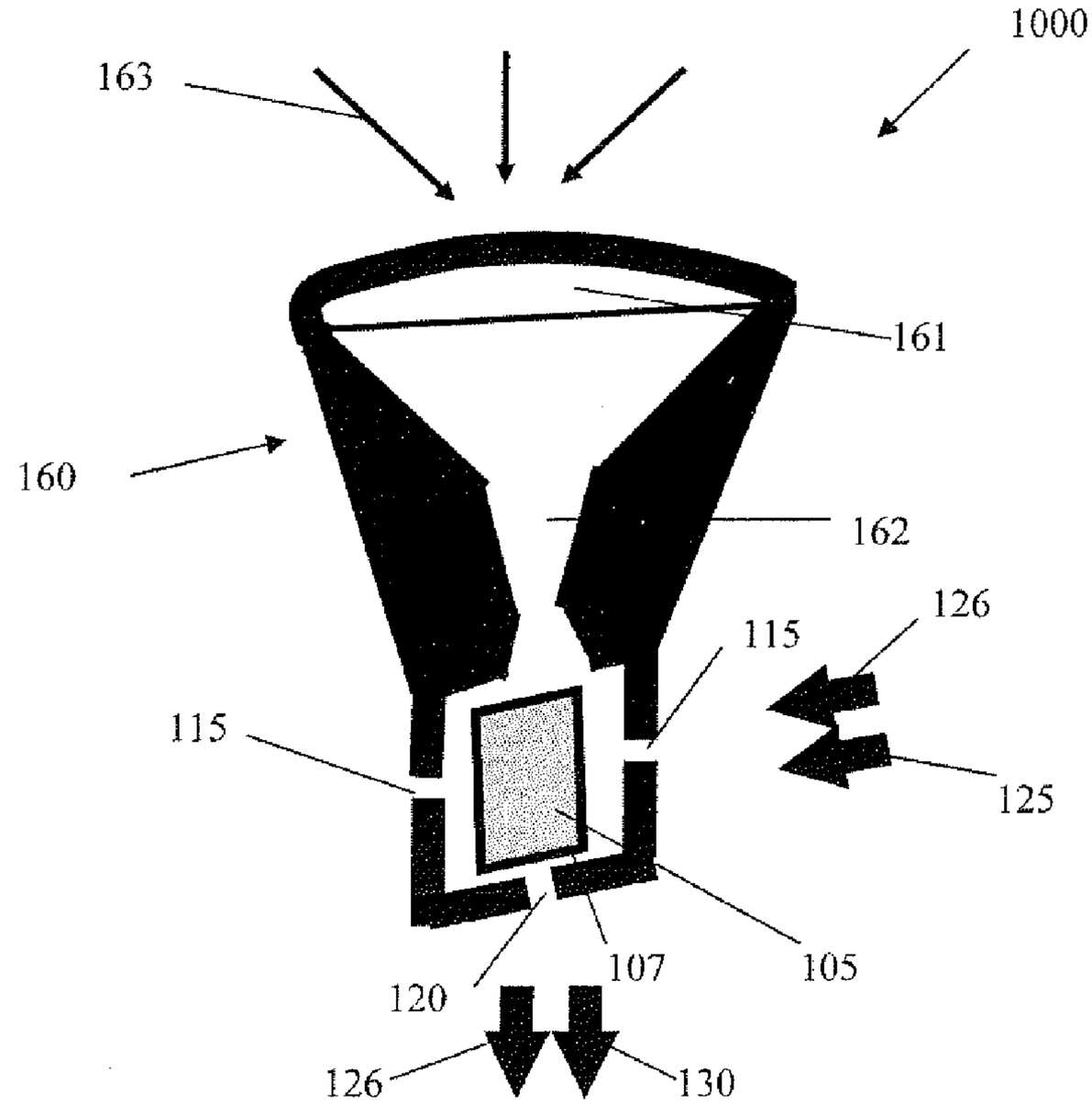

FIG. 10

Material	Crystallite Size (nm)	
	As-made	Cycled
3 DOM CeO_2-PM	7.4	73.8
3 DOM $Ce_{0.9}Zr_{0.1}O_2$-PM	5.1	18.2
3 DOM $Ce_{0.8}Zr_{0.2}O_2$-PM	4.1	14.8
3 DOM $Ce_{0.7}Zr_{0.3}O_2$-PM	5.5	11.6
3 DOM $Ce_{0.6}Zr_{0.4}O_2$-PM	4.4	10.6
3 DOM $Ce_{0.5}Zr_{0.5}O_2$-PM	5.9	9.7

FIG. 11

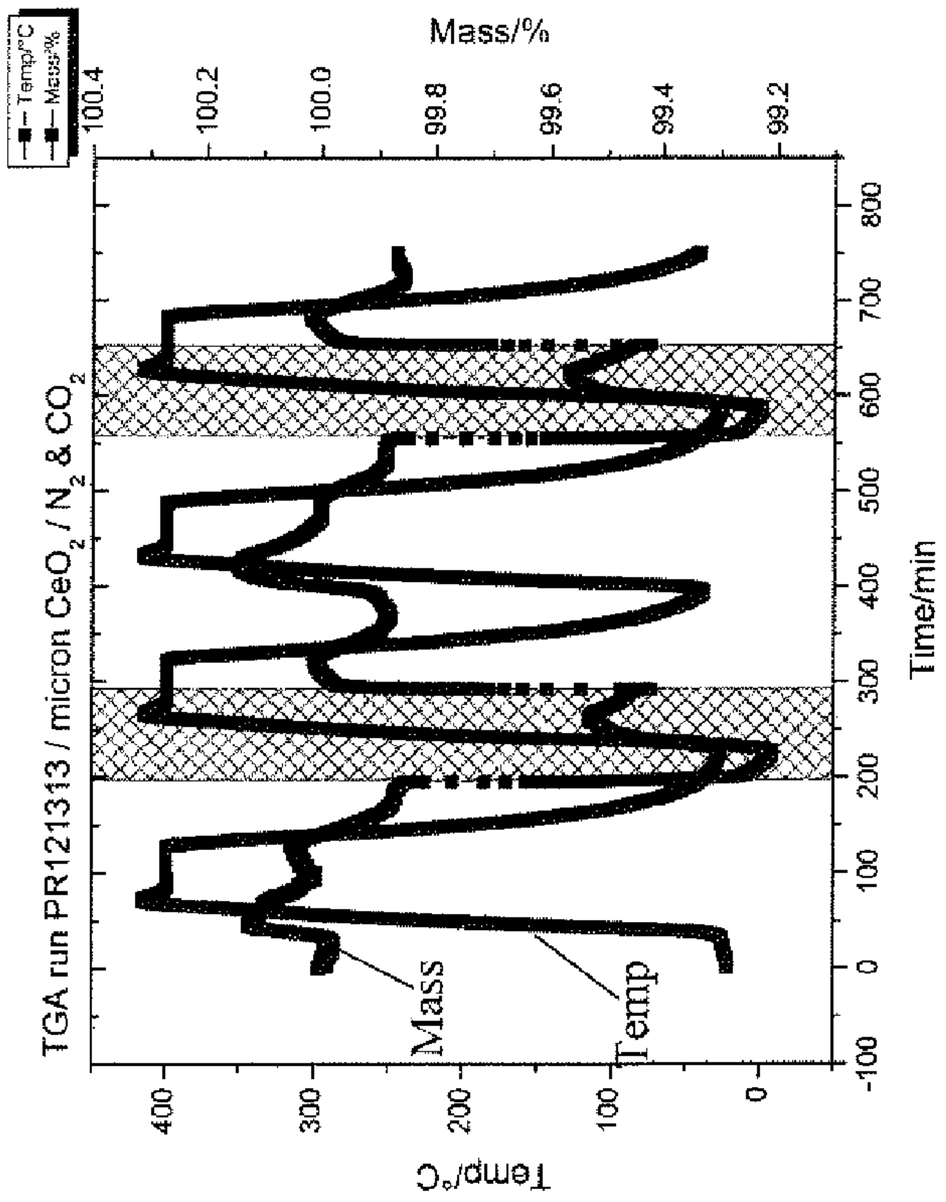

FIG. 12B

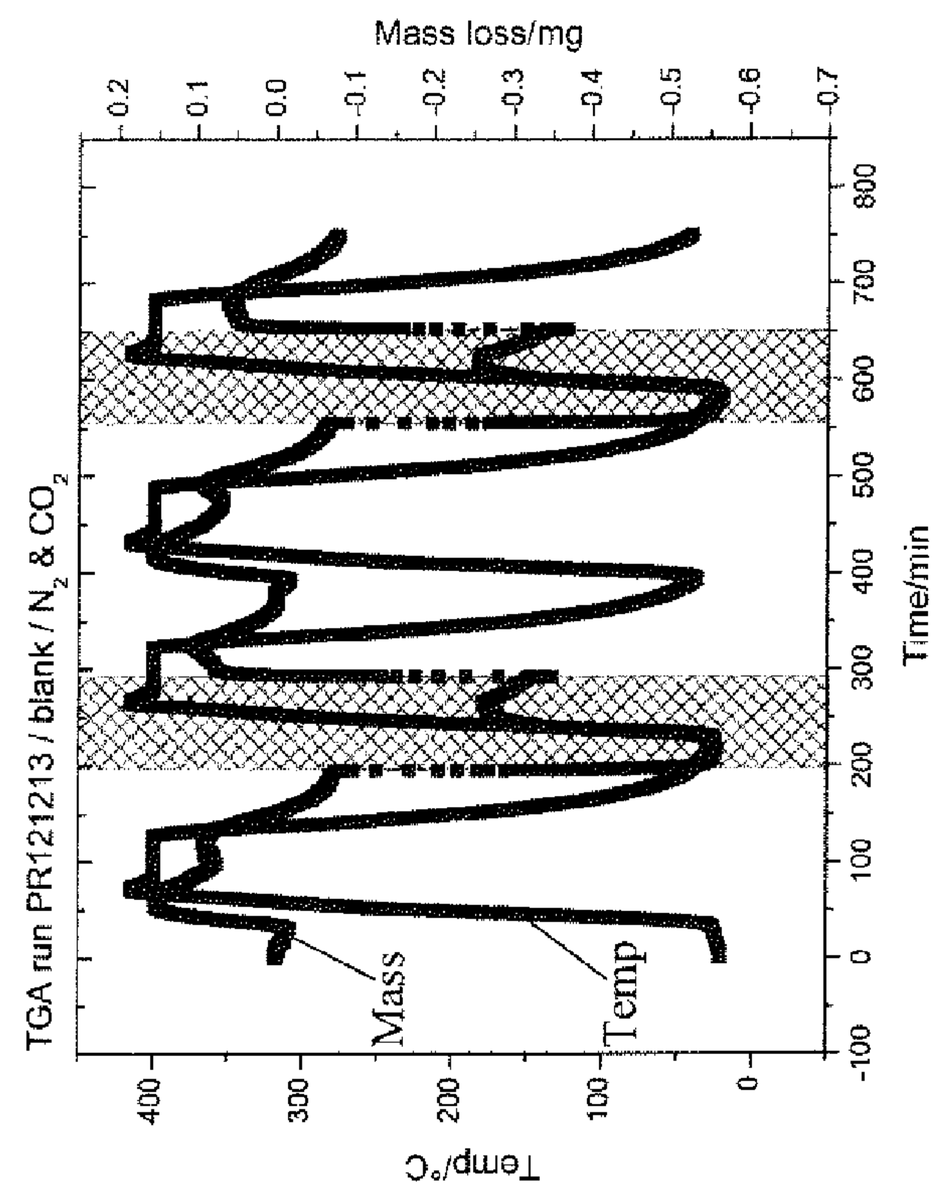

FIG. 12A

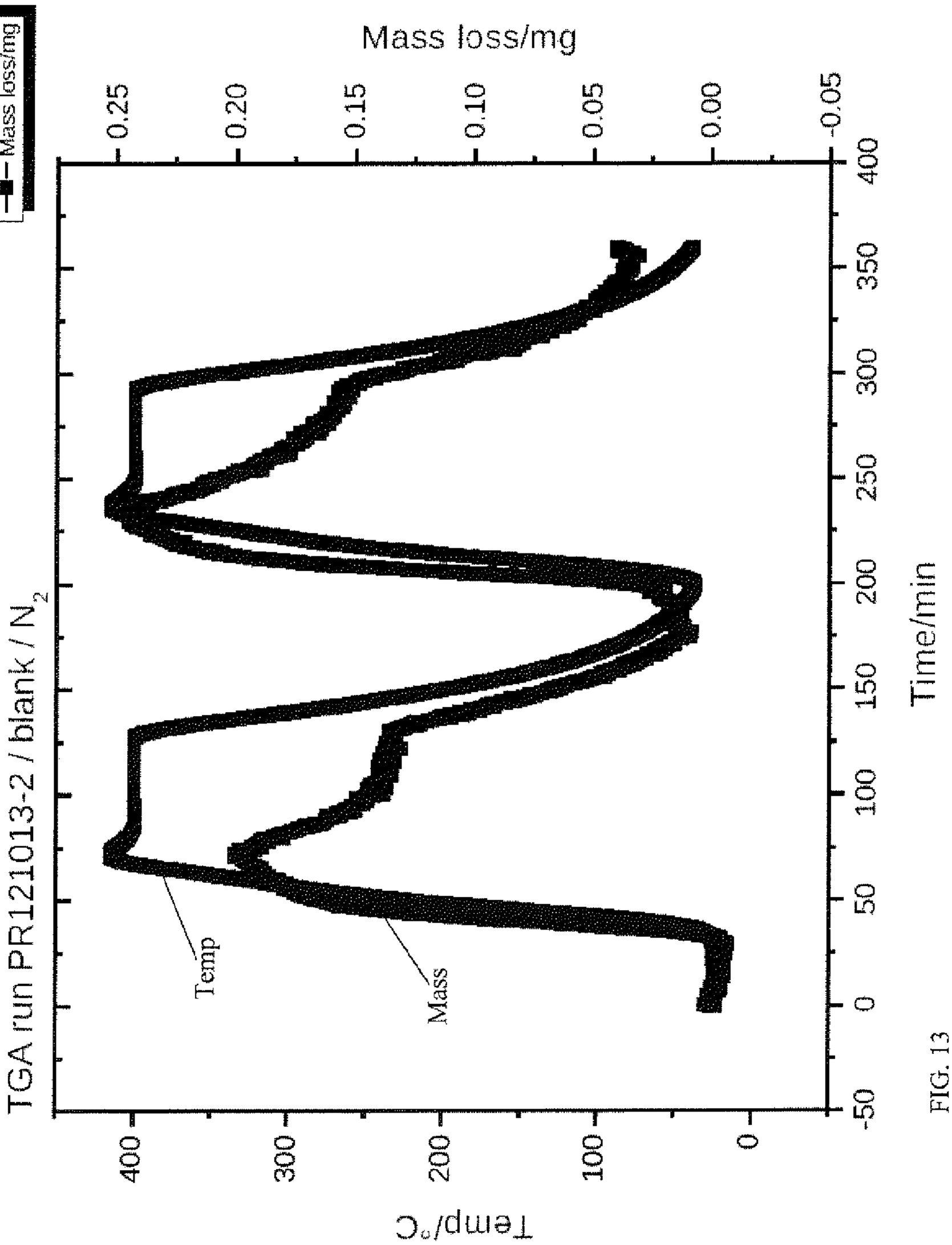
TGA run PR121013-2 / blank / N2
Temp/°C
Mass loss/mg
Temp
Mass
Mass loss/mg
0.25
0.20
0.15
0.10
0.05
0.00
-0.05
400
350
300
250
200
150
100
50
0
-50
Time/min
400
300
200
100
0
Temp/°C

FIG. 13

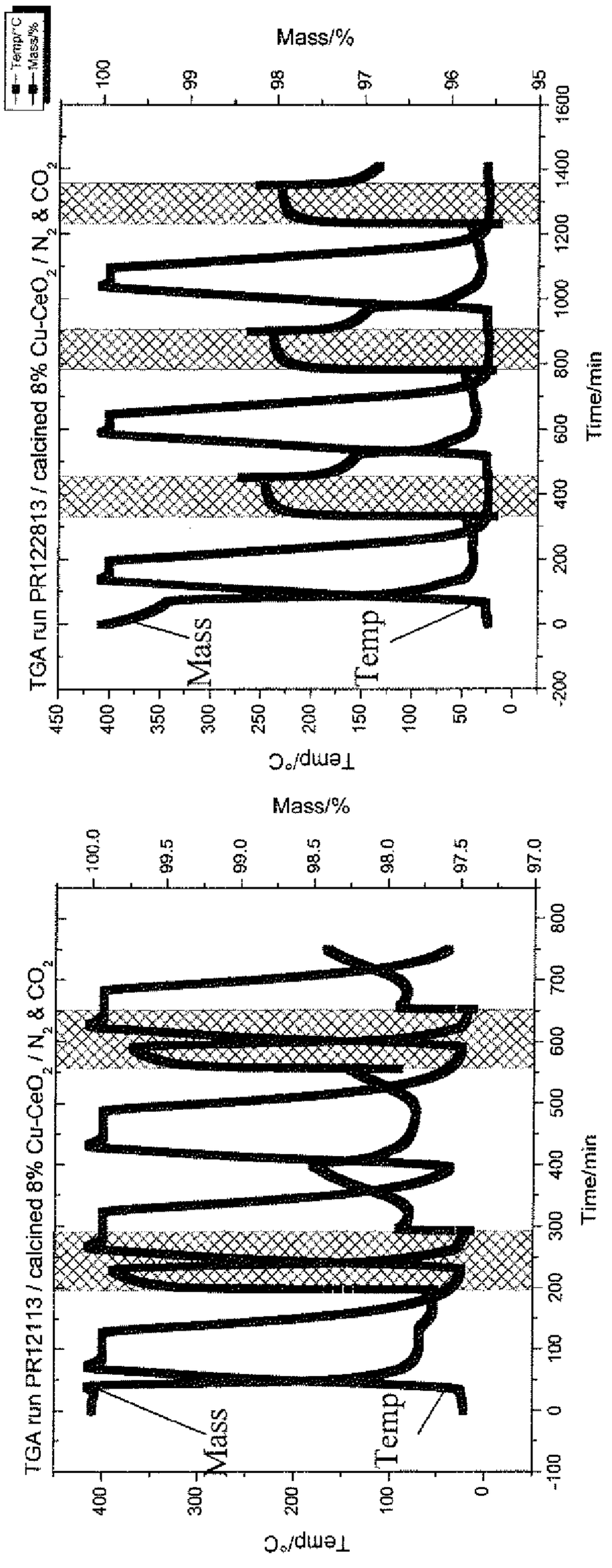

FIG. 14B

FIG. 14A

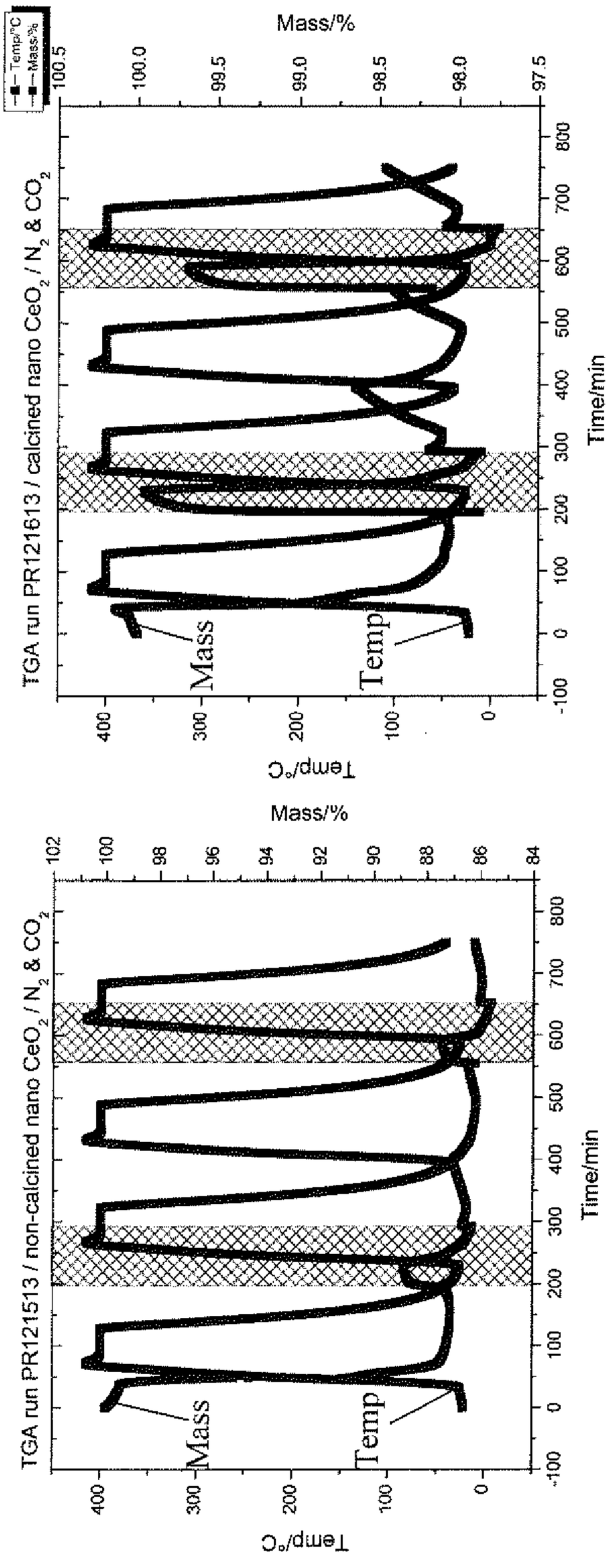

FIG. 15B

FIG. 15A

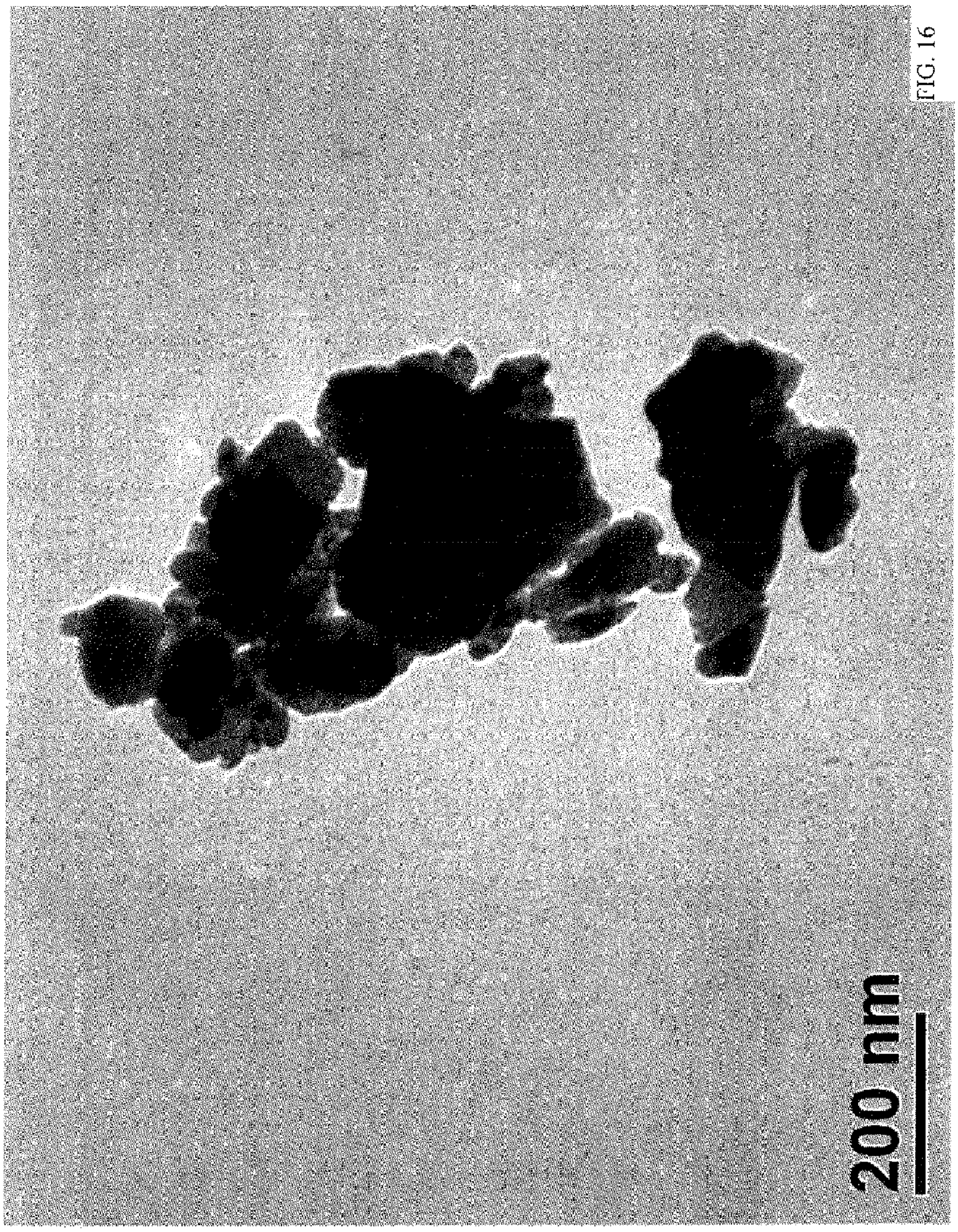

FIG. 16

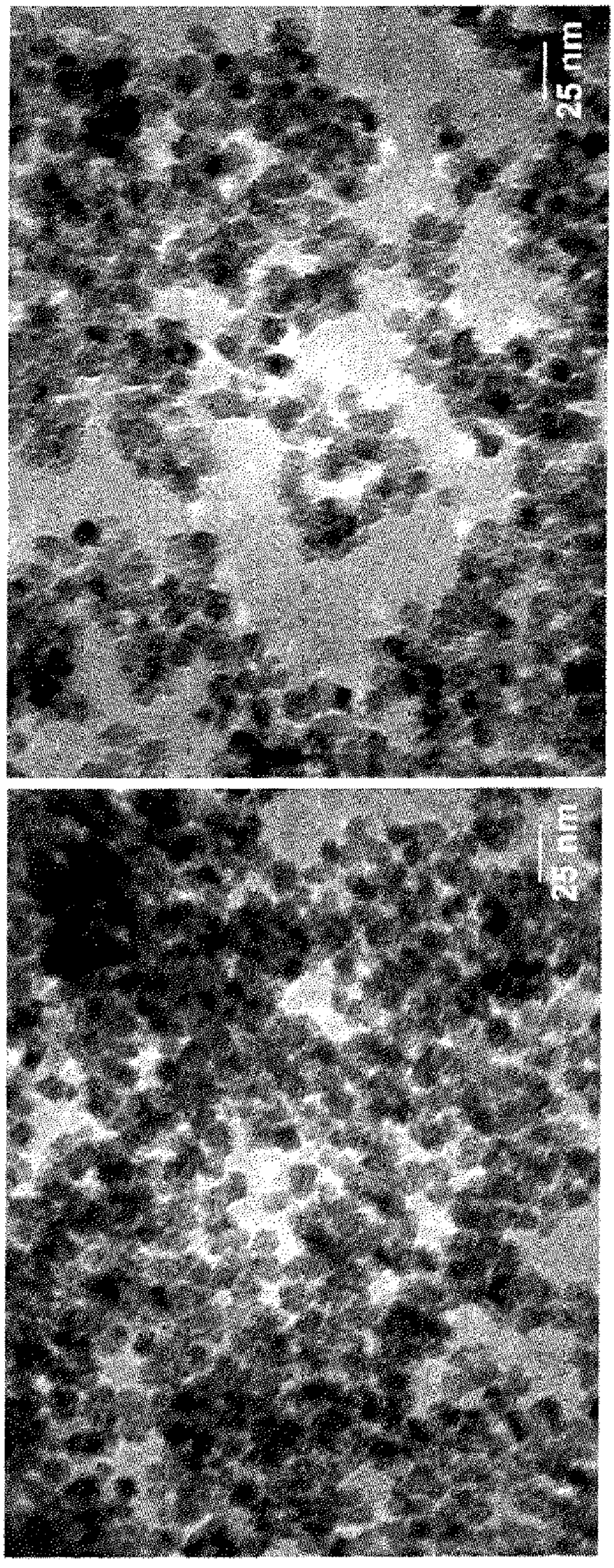

FIG. 17B

FIG. 17A

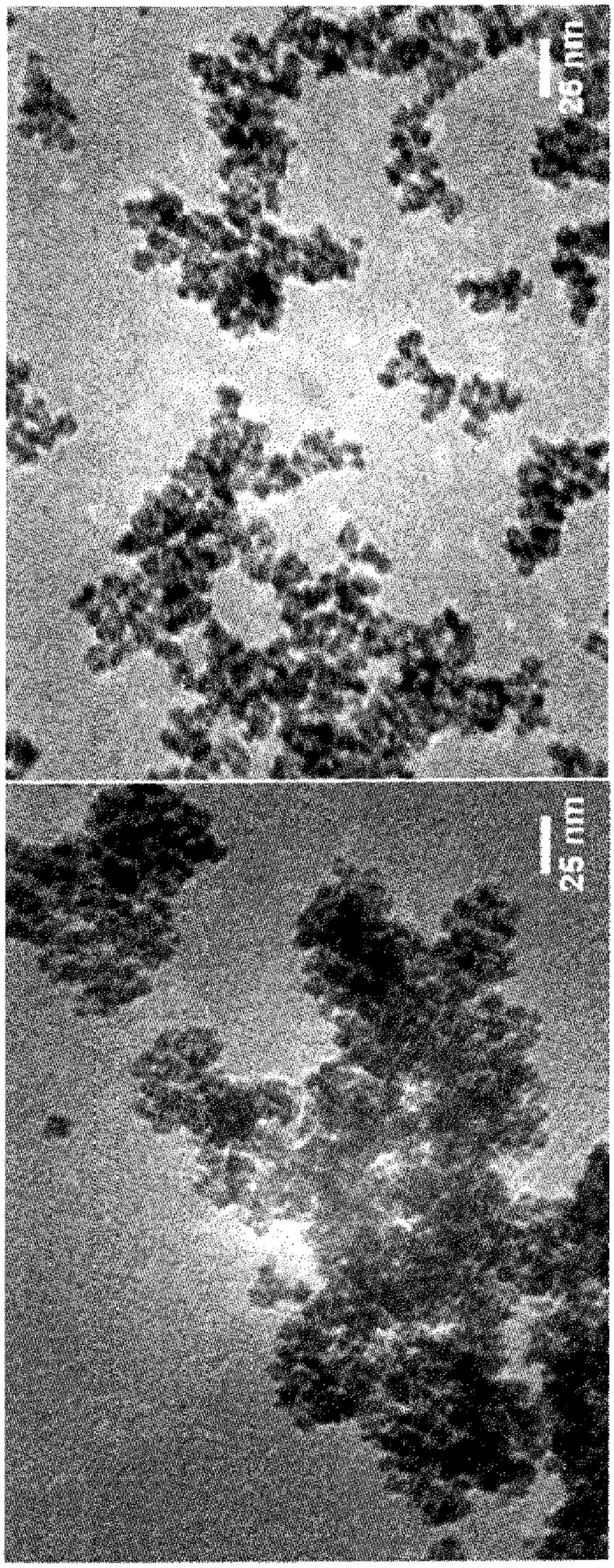

FIG. 18B

FIG. 18A

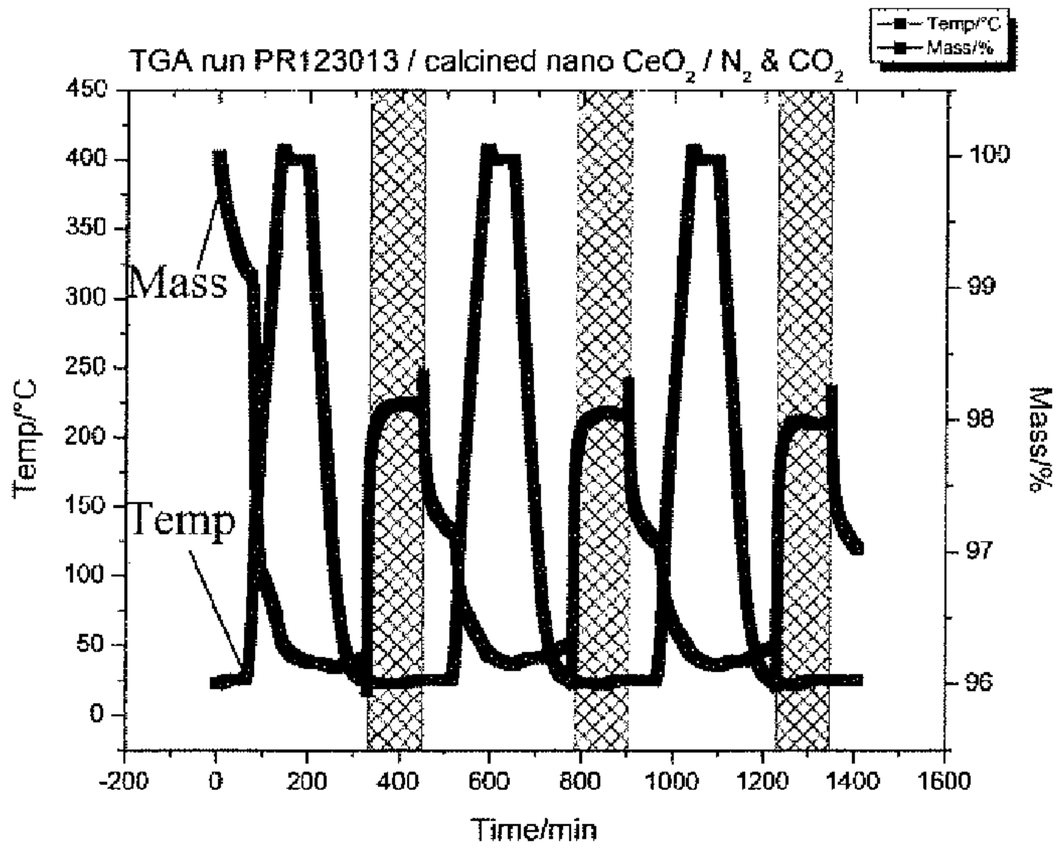

FIG. 19A

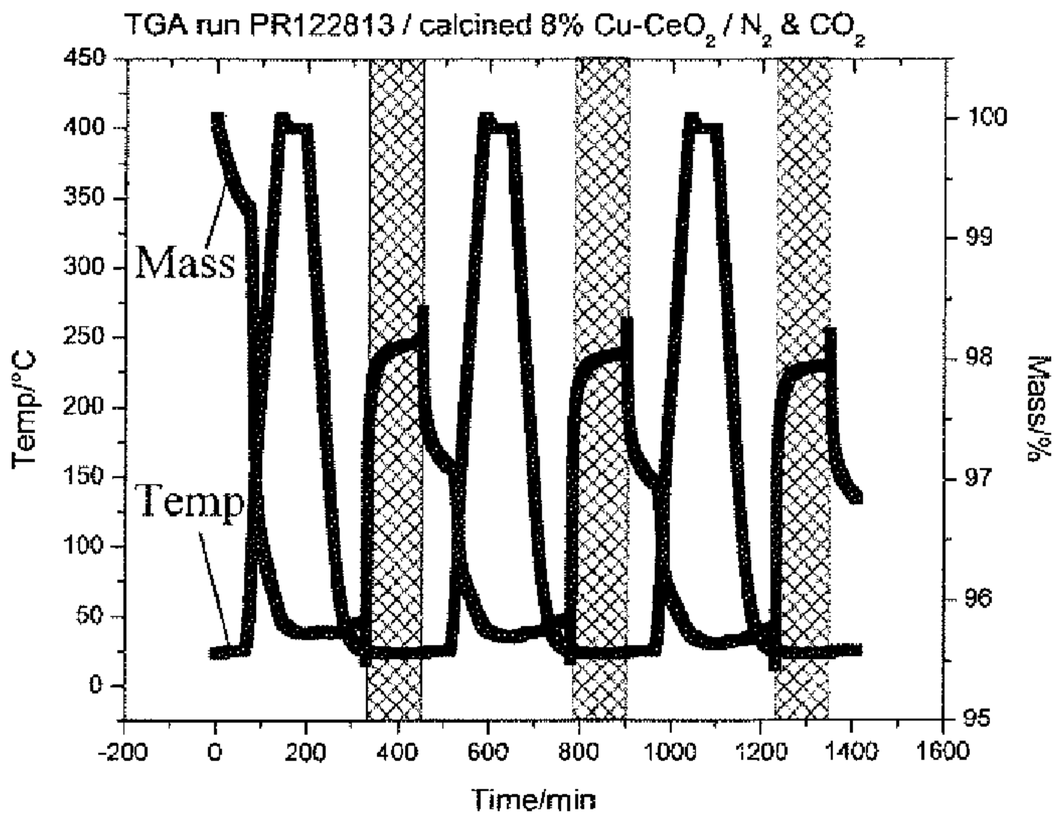

FIG. 19B

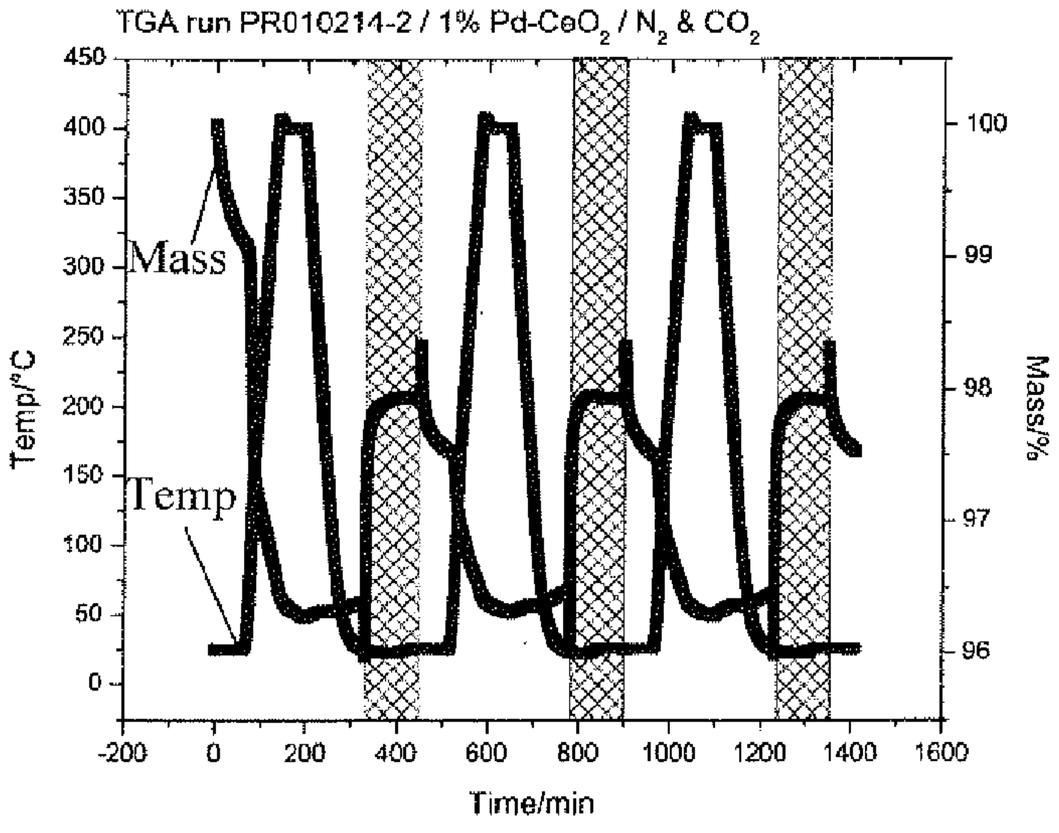

FIG. 19C

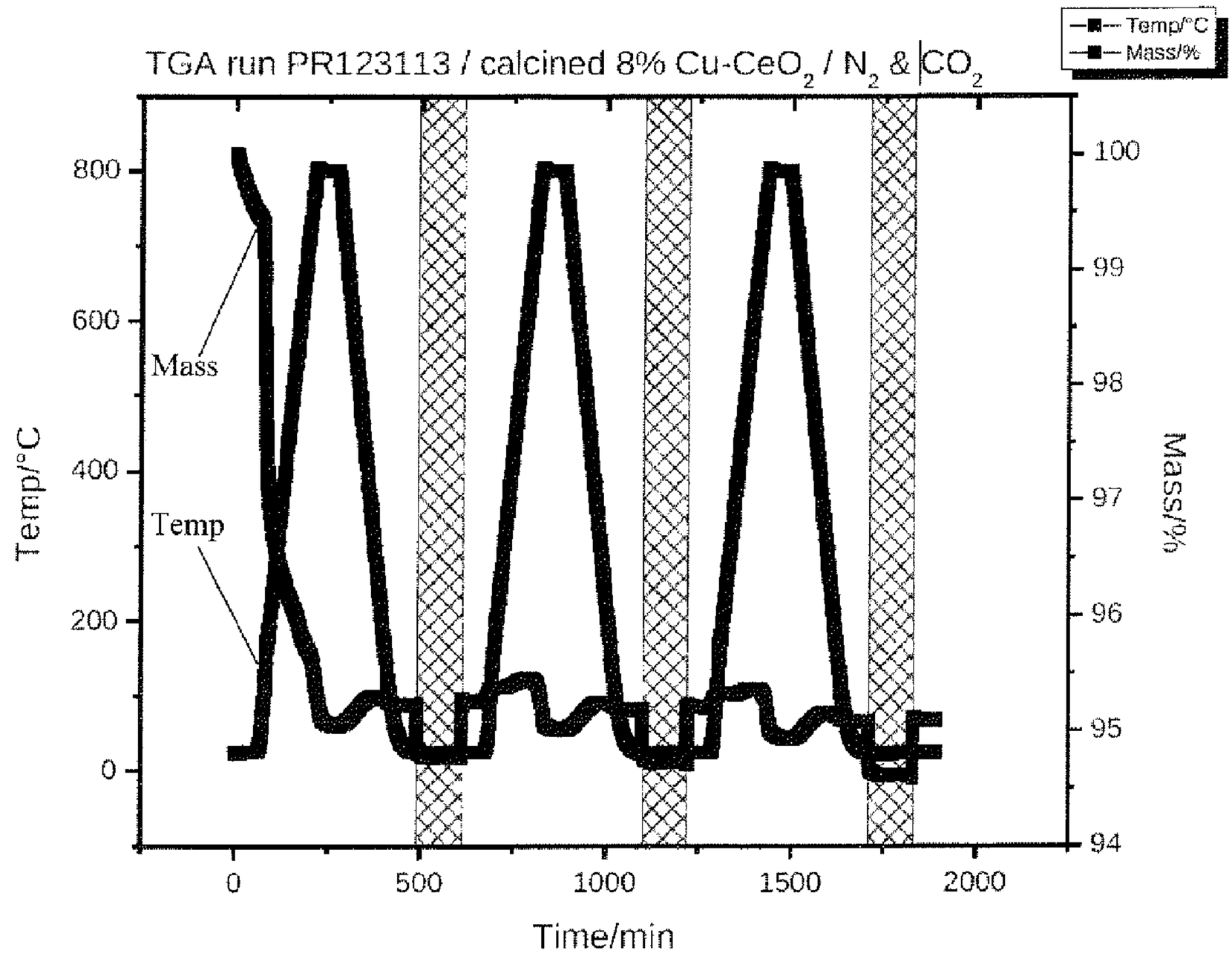
TGA run PR123113 / calcined 8% Cu-CeO2 / N2 & CO2
Temp/°C
Mass/%
800
600
400
200
0
Mass
Temp
Temp/°C
100
99
98
97
96
95
94
Mass/%
0
500
1000
1500
2000
Time/min

FIG. 20

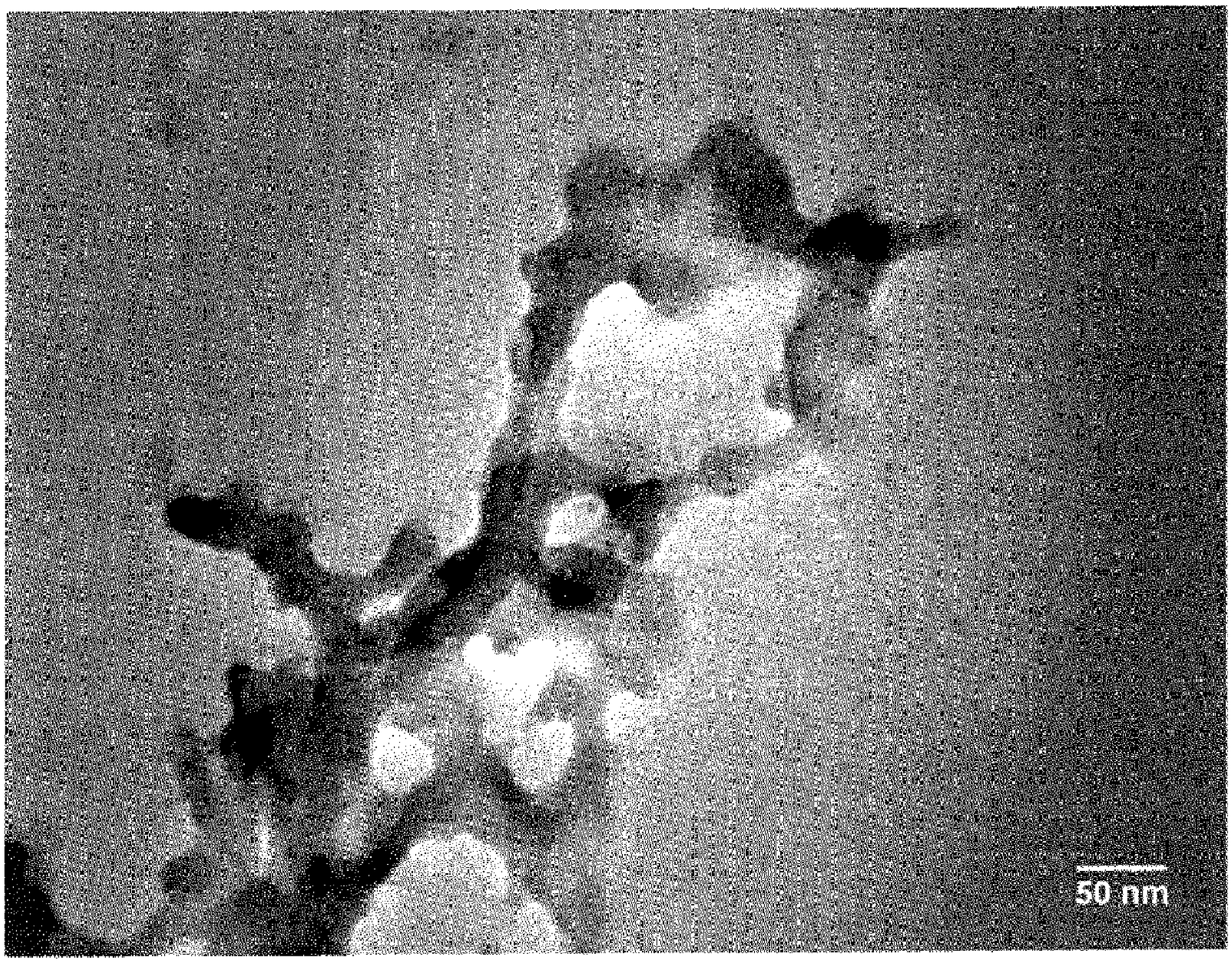

FIG. 21

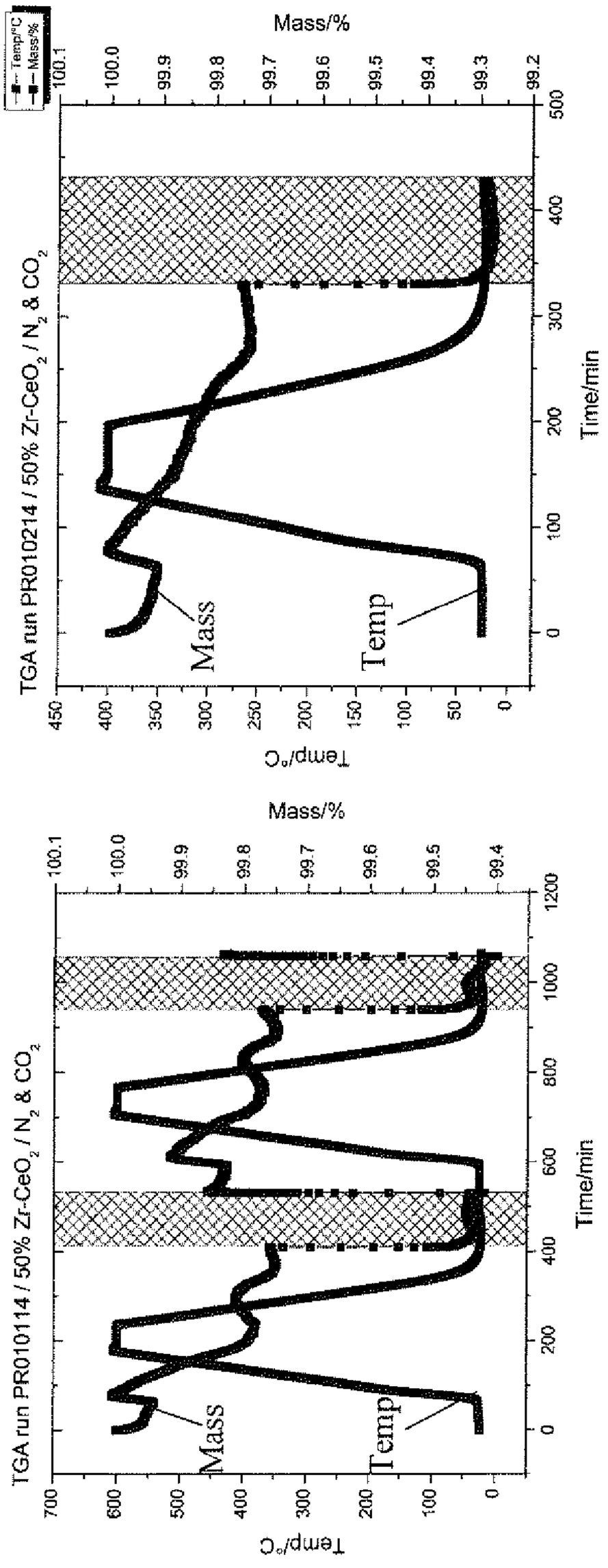

FIG. 22B

FIG. 22A

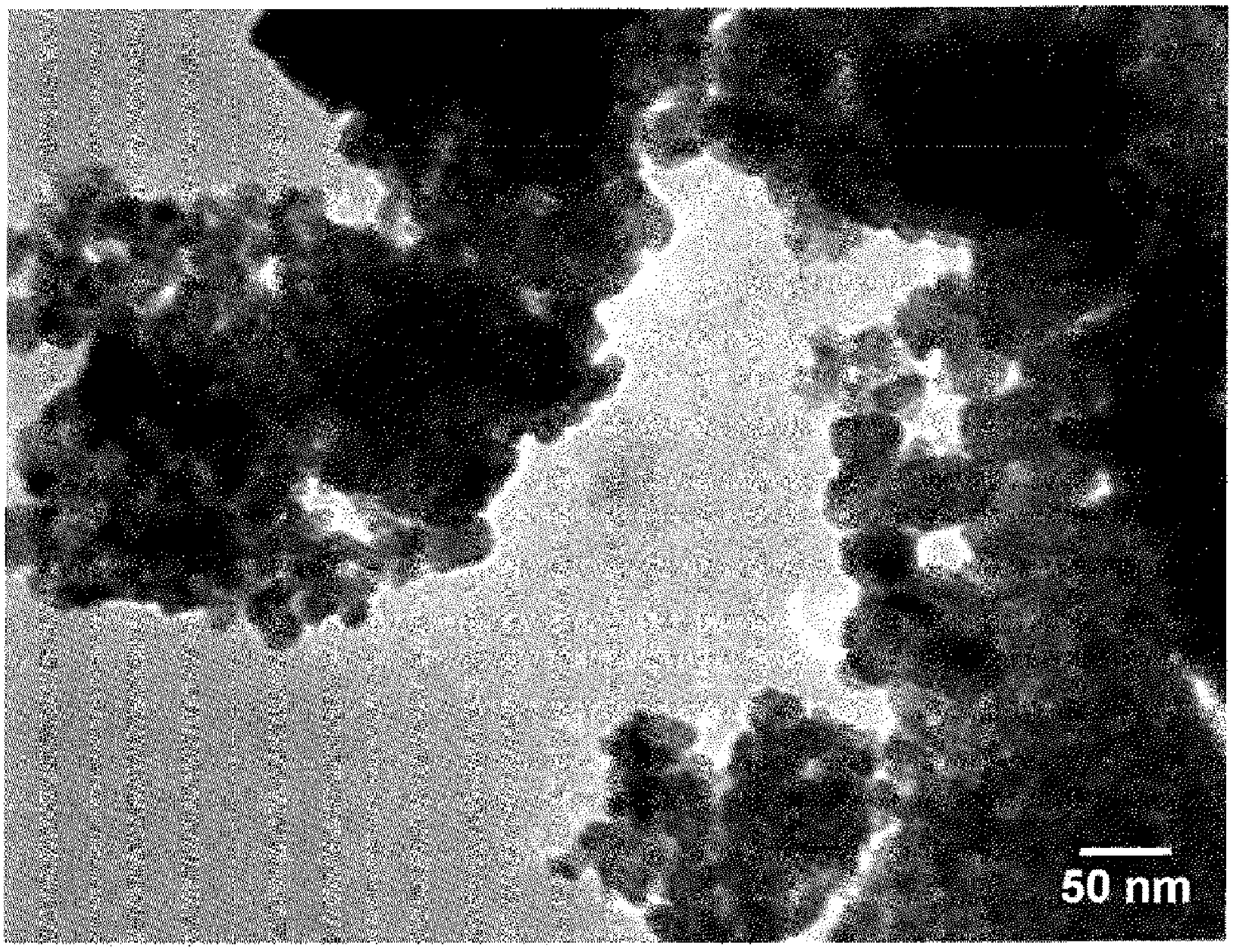

FIG. 23

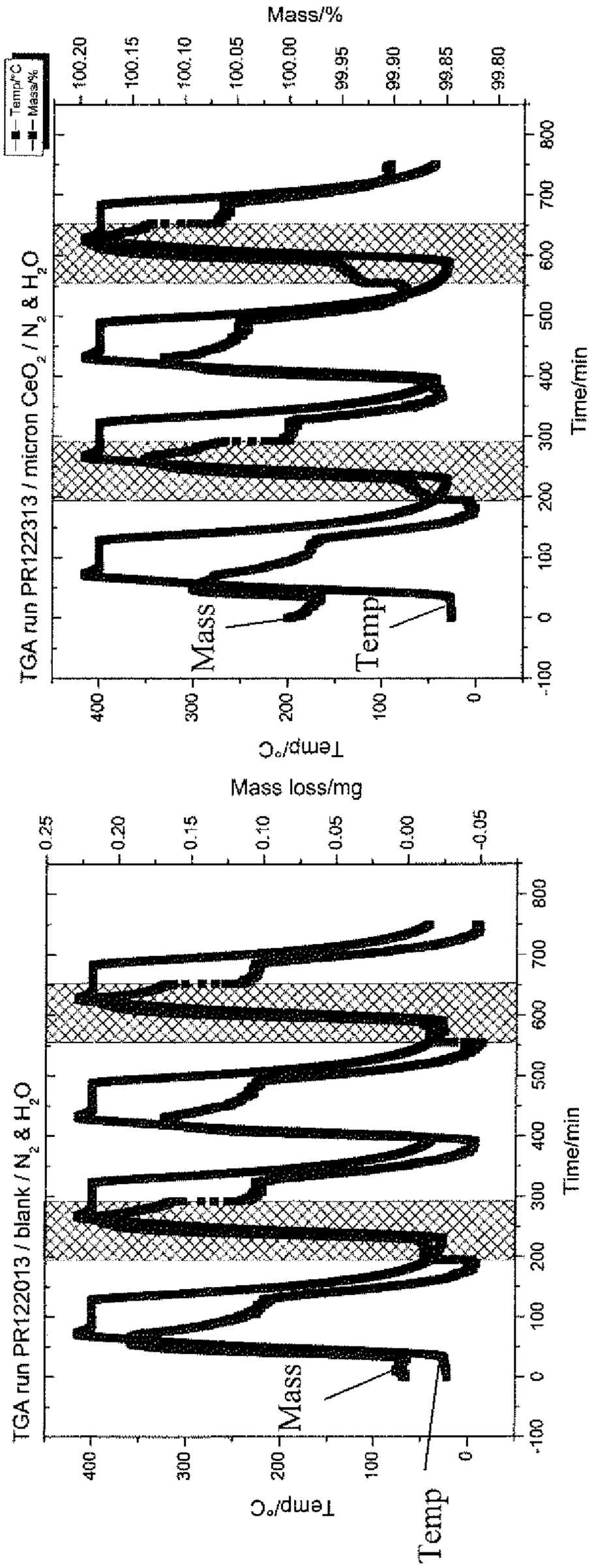

FIG. 24B

FIG. 24A

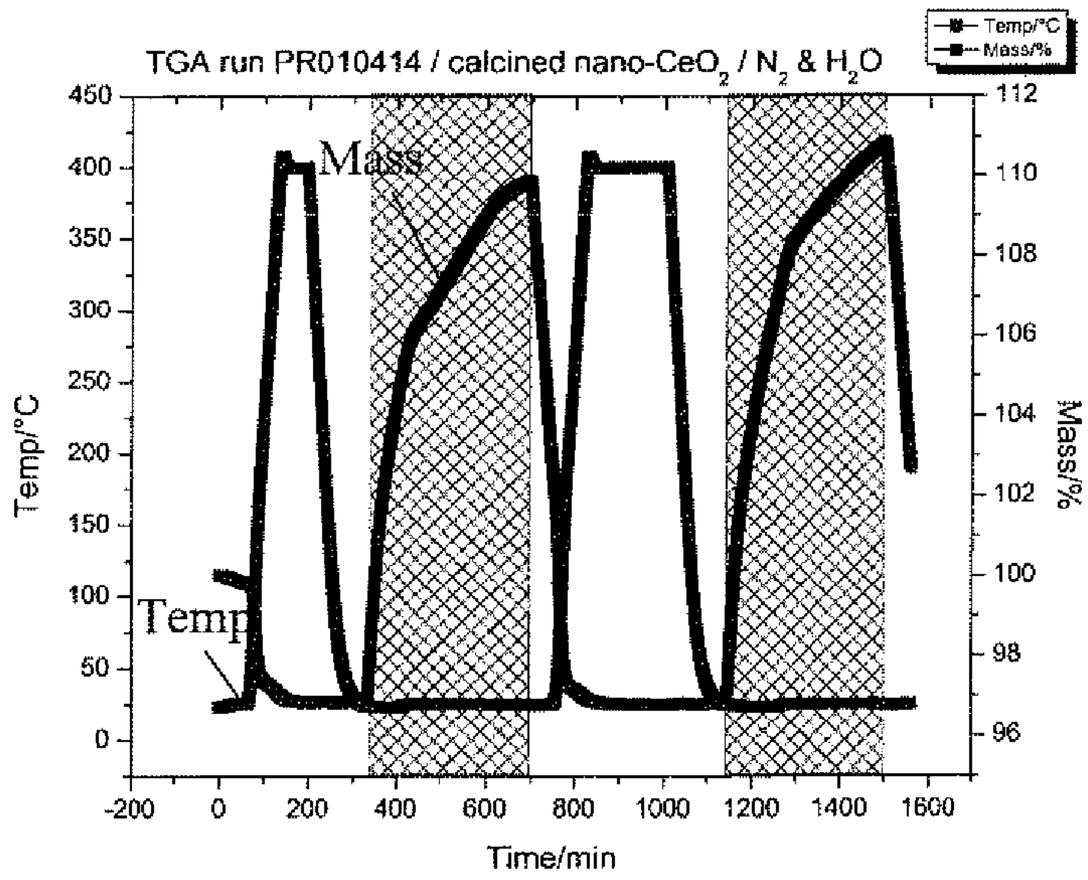

FIG. 25A

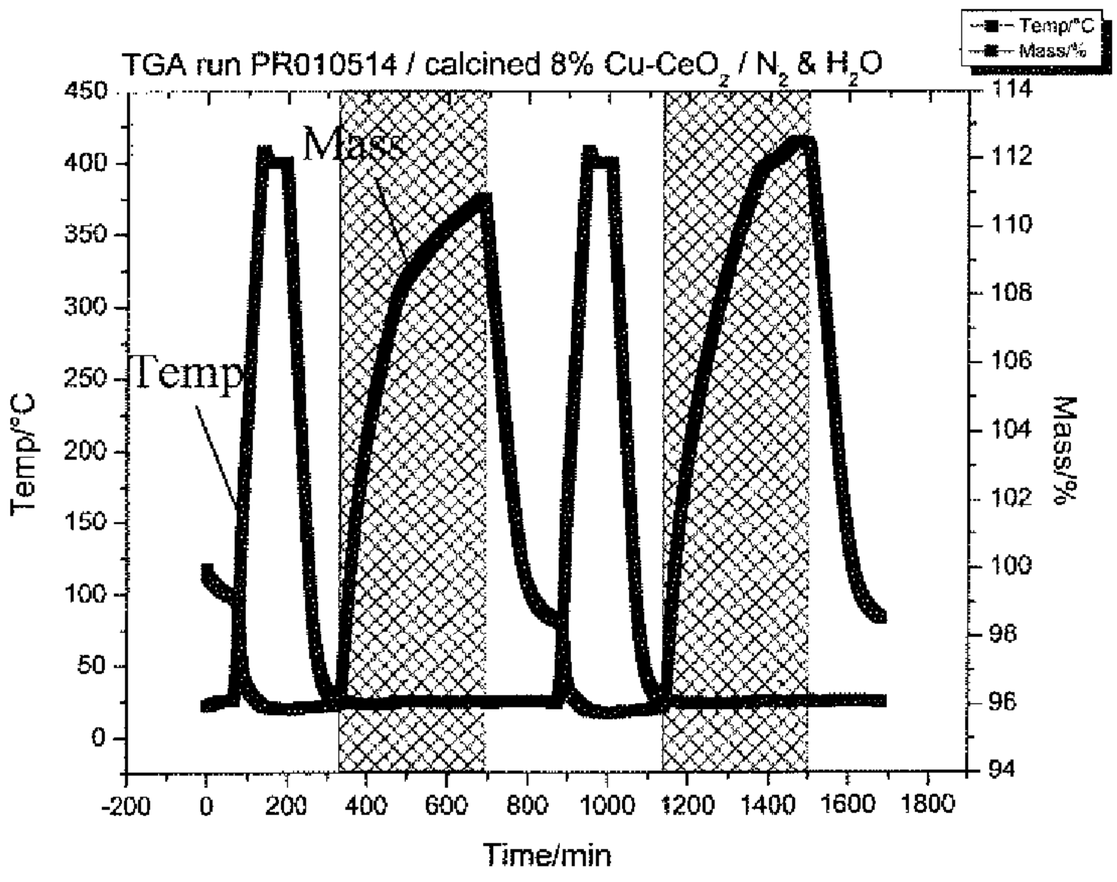

FIG. 25B

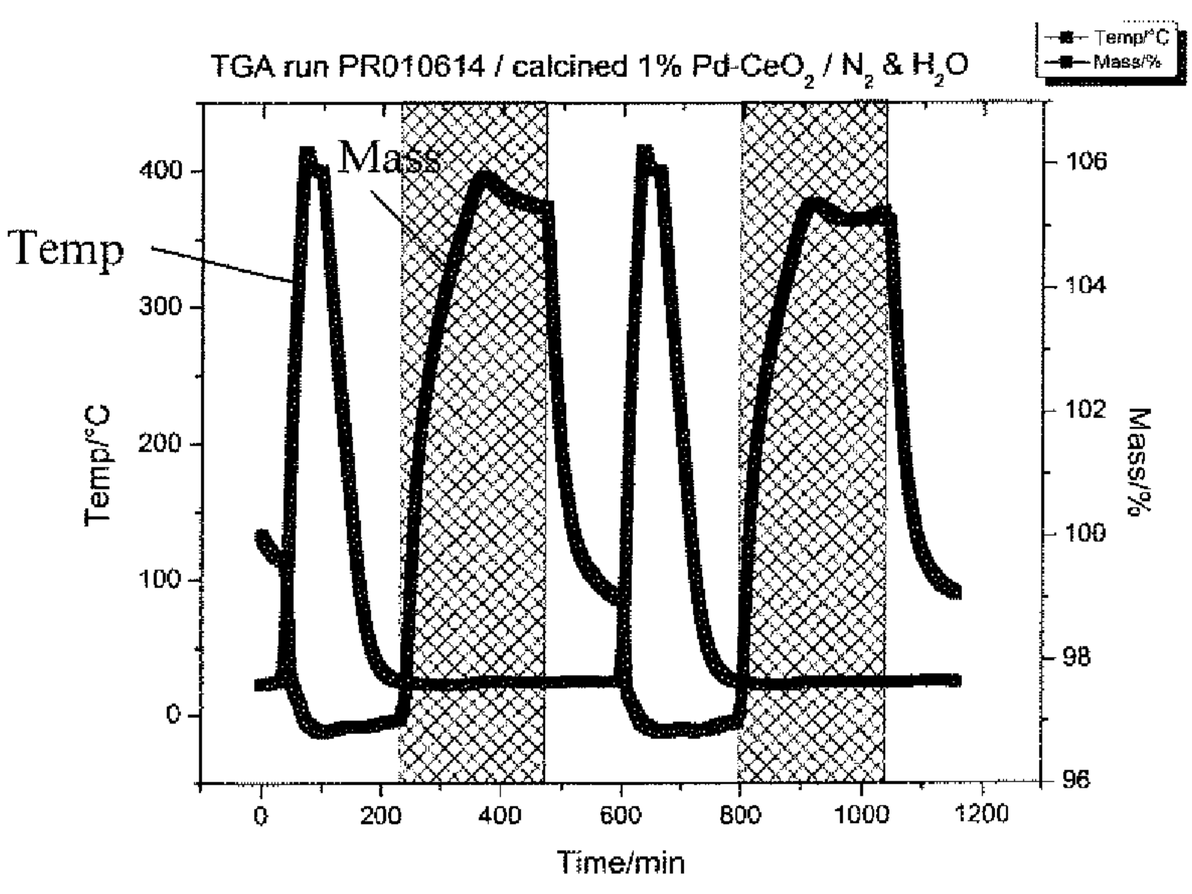

FIG. 25C

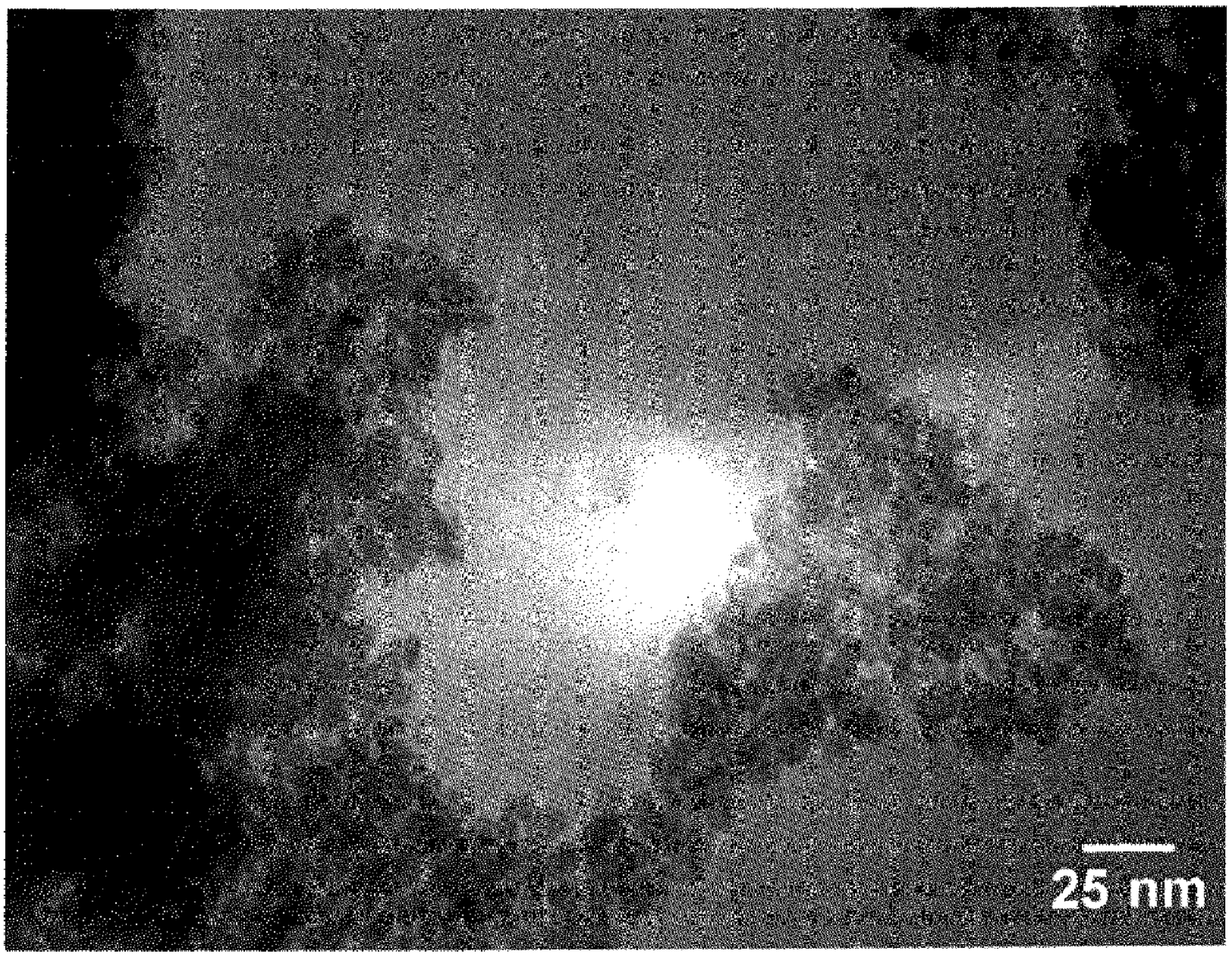

FIG. 26

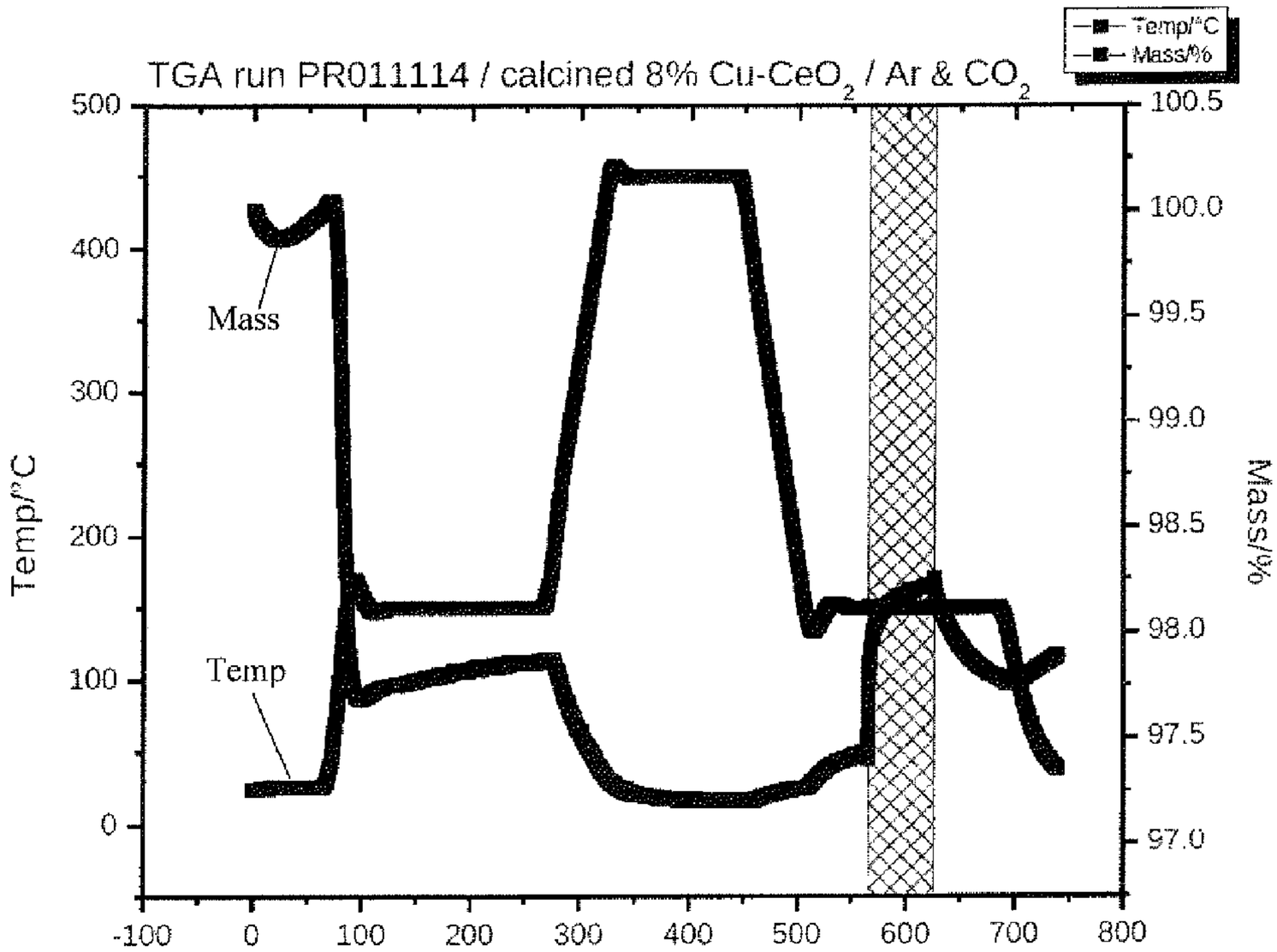
TGA run PR011114 / calcined 8% Cu-CeO2 / Ar & CO2
Temp/°C
Mass/%
Mass
Temp
Temp/°C
Mass/%
Time/min
500
400
300
200
100
0
100.5
100.0
99.5
99.0
98.5
98.0
97.5
97.0
-100
0
100
200
300
400
500
600
700
800

FIG. 27

METHOD AND SYSTEM FOR PRODUCTION OF HYDROGEN AND CARBON MONOXIDE

CROSS REFERENCE TO RELATED APPLICATIONS

[0001] This application is a continuation-in-part of International Patent Application No. PCT/US2012/047303, filed Jul. 19, 2012, which claims priority from U.S. Provisional Application No. 61/509,370, filed Jul. 19, 2011 and U.S. Provisional Application No. 61/638,960, filed Apr. 26, 2012, the disclosure of each of which is herein incorporated by reference by its entirety.

BACKGROUND

[0002] Converting H_2O and CO_2 gases into syngas (H_2 and CO) can be a useful strategy for carbon sequestration and as a source of renewable energy. One technique for realizing energy conversion involves heating porous monolithic cerium dioxide (ceria) to about 1600° C. to release oxygen from the micron-sized (bulk) crystals/grains. When the resulting reduced ceria is cooled, H_2O or CO_2 can be converted to H_2 and CO, respectively, while ceria is re-oxidized and ready for another thermal-gas cycle. This high reduction temperature of about 1600° C. is dictated by the reduction thermodynamics of bulk ceria (i.e. ceria grains in micron-size and larger). However, the high temperature can increase the cost of the process and reduce material lifetime. Therefore, it is desirable to lower the ceria reduction temperature to improve the economics and material stability of the process.

SUMMARY

[0003] The disclosed subject matter provides techniques for preparing a fuel using an oxygen-storing compound. In accordance with one aspect of the disclosed subject matter, methods of preparing a fuel using an oxygen-storing compound in the form of nanoparticles is provided. An exemplary method includes heating the nanoparticles at a first temperature to release an amount of oxygen, thus producing a reduced oxide compound, and exposing the reduced oxide compound to gaseous carbon dioxide and/or water vapor at a second temperature to produce CO and/or H_2, which are also referred as the gaseous fuel, or fuel. As liquid fuels such as gasoline and diesel oil can be prepared from CO and H_2, the mixture of CO and H_2 is also referred as syngas. The first temperature can be about 700° C. or lower, 450° C. or lower, or 300° C. or lower (e.g., between about 150° C.-300° C.). The second temperature can be, but not necessarily be, lower than the first temperature. The fuel can include at least one of carbon monoxide and molecular hydrogen, or mixture thereof.

[0004] The oxygen-storing compound nanoparticles can include cerium oxide (ceria) nanoparticles. The oxygen-storing compound can be cerium oxide doped with one or more transition metals, such as Cu, Zr, Pd, Hf, Fe, Cr, Co, Zn, Ni, Au, Ti, Pt, Rh, and Ru, as well as a rare earth metal such as Y, Gd, and the like. The oxides of these metals can also be used as dopants. In some embodiments, the transition metal is Cu. The amount of Cu can be such that it replaces about 0.01 to about 0.16 of cerium in the ceria, or about 0.05 to about 0.10, or about 0.08 of cerium (cation-atomic ratio). The oxygen-storing compound nanoparticles can have an average size (diameter) of about 1 to about 100 nm, about 2 to about 50 nm, about 2 to about 20 nm, about 2 to about 15 nm, 5 to about 15 nm, and about 5 to about 10 nm.

[0005] In accordance with one aspect of the disclosed subject matter, a system for preparing a fuel from a gas using nanoparticles of an oxygen-storing compound is provided. The system includes a reactor adapted to hold nanoparticles of the oxygen-storing compound in a predetermined location and to receive the gas through a gas intake, and a heater adapted to heat the oxygen-storing compound nanoparticles to a first temperature to reduce the nanoparticles to form a reduced oxygen-storing compound. The oxygen-storing nanoparticles can be thermally reduced at the first temperature, and then an oxygen-carrying gas such as CO_2 and/or H_2O can be introduced through the gas intake to react with the reduced nanoparticles at a second temperature to form the fuel. The fuel can be carbon monoxide, molecular hydrogen, or mixture thereof. The heater can be a passive heater or exchanger, coupled with a heat source having a temperature of about 700° C. or lower, 450° C. or lower, or 300° C. or lower. Additionally or alternatively, the heat source can have a temperature of at least 150° C., for example, a temperature of 150-300° C. The heat source can be waste heat (e.g., in the form of a flue gas) from an industrial process or facility, for example, a refinery, a chemical plant, a nuclear plant or other power plants. Alternatively, the heater can utilize coal-burning, electric or other forms of energy, such as being coupled with a solar concentration device. The oxygen-storing compound nanoparticles can be ceria doped with one or more metals, as described above.

BRIEF DESCRIPTION OF THE DRAWINGS

[0006] FIG. **1** is a diagram depicting an example system for preparing a fuel from a gas using nanoparticles of an oxygen-storing compound according to the disclosed subject matter.

[0007] FIG. **2** is a plot showing the relationship between lattice parameter of CeO_2 nanoparticles and the size of the CeO_2 nanoparticles.

[0008] FIG. **3** is a plot of H_2-Temperature Program Reduction (TPR) results of Cu—CeO_2 nanoparticle samples having different loading levels of Cu (1.6%, 8.2% and 19.6%). The area under the peak corresponding to the amount of H_2 converted to H_2O by the oxygen in the sample. The larger the area under the curve means a larger reduction capacity of the sample. Temperature program simply means a constant heating rate.

[0009] FIG. **4** is a plot showing the results of a thermogravimetric analysis (TGA) of a sample of Cu—CeO_2 nanoparticles.

[0010] FIG. **5** is a plot showing the time course of the temperature and the weight of a sample of Cu—CeO_2 nanoparticles during a TGA test.

[0011] FIG. **6** is a TGA plot of a sample of undoped CeO_2 nanoparticles.

[0012] FIG. **7** is a TGA plot of a sample of Zr—CeO_2 nanoparticles.

[0013] FIG. **8** is a plot showing the changes in the lattice parameter and particle size of a nano ceria sample having a starting average size of 6.7 nm when the sample is heated.

[0014] FIG. **9** is a diagram depicting an example support structure for supporting nanoparticles of an oxygen-storing compound according to some embodiments of the disclosed subject matter.

[0015] FIG. **10** is a diagram depicting an example system for preparing a fuel from a gas using nanoparticles of an oxygen-storing compound according to the disclosed subject matter.

[0016] FIG. **11** is a chart depicting anticoarsening effects of zirconia doping on ceria according to some embodiments of the disclosed subject matter.

[0017] FIG. **12**A is a diagram depicting an exemplary blank run and FIG. **12**B is a diagram depicting an exemplary run of micron ceria under identical thermogravimetric analysis (TGA) conditions according to some embodiments of the disclosed subject matter.

[0018] FIG. **13** is a diagram depicting an exemplary blank TGA run with only N_2 flow according to some embodiments of the disclosed subject matter.

[0019] FIGS. **14**A and **14**B are diagrams depicting exemplary runs of calcined 8% Cu—CeO_2 under different TGA experimental conditions according to some embodiments of the disclosed subject matter.

[0020] FIGS. **15**A and **15**B are diagrams depicting exemplary runs of nano ceria (non-calcined and calcined, respectively) under identical TGA conditions according to some embodiments of the disclosed subject matter.

[0021] FIG. **16** is a transmission electron microscope (TEM) image of exemplary commercial micron ceria according to some embodiments of the disclosed subject matter.

[0022] FIG. **17**A is an exemplary TEM image of PR-IV-23-A ceria, made with hexamethylenetetramine (HMT) and no heat annealing, and FIG. **17**B is an exemplary TEM image of the same sample treated at 400° C. overnight (PR-IV-35-C ceria), according to some embodiments of the disclosed subject matter.

[0023] FIG. **18**A is an exemplary TEM image of a sample (HS-I-19-A) that has not been heat annealed, and FIG. **18**B is an exemplary TEM image of the same sample after being heat annealed at 400° C. overnight (PR-IV-34-A), according to some embodiments of the disclosed subject matter.

[0024] FIGS. **19**A, **19**B, and **19**C are diagrams depicting exemplary CO_2 TGA runs of nan oceria, copper-doped ceria, and palladium-doped ceria, respectively, according to some embodiments of the disclosed subject matter.

[0025] FIG. **20** is a diagram depicting an exemplary TGA run of copper-doped ceria, according to some embodiments of the disclosed subject matter.

[0026] FIG. **21** is an exemplary TEM image of copper-doped ceria after TGA cycling up to 800° C. (PR-IV-41-A), according to some embodiments of the disclosed subject matter.

[0027] FIGS. **22**A and **22**B are diagrams depicting exemplary TGA runs of zirconia-doped ceria according to some embodiments of the disclosed subject matter.

[0028] FIG. **23** is an exemplary TEM image of 50/50 zirconia-ceria nanoparticles according to some embodiments of the disclosed subject matter.

[0029] FIGS. **24**A and **24**B are diagrams depicting exemplary runs of N_2/H_2O TGA cycling up to 400° C. with blank (FIG. **24**A) and micron CeO_2 (FIG. **24**B) according to some embodiments of the disclosed subject matter.

[0030] FIGS. **25**A, **25**B, and **25**C are diagrams depicting exemplary H_2O TGA runs of nano ceria, copper-doped ceria, and palladium-doped ceria, respectively, according to some embodiments of the disclosed subject matter.

[0031] FIG. **26** is an exemplary TEM image of 8% Cu-ceria after N_2/H_2O TGA treatment (PR-IV-34-A), according to some embodiments of the disclosed subject matter.

[0032] FIG. **27** is a diagram depicting exemplary TGA cycling between 150° C. and 450° C., according to some embodiments of the disclosed subject matter.

DETAILED DESCRIPTION

[0033] The disclosed subject matter provides methods and systems for preparing a fuel, such as H_2 and/or CO, using oxygen-storing compound nanoparticles. The process involves reducing the oxygen-storing compound nanoparticles at a first temperature, e.g., by heating, and exposing the reduced nanoparticles to a gas including CO_2 and/or water vapor to produce the fuel. Upon reacting with the gas, the reduced nanoparticles are oxidized and the original oxygen-storing compound can be restored. As will be further described below, because the reduction of the oxygen-storing compound nanoparticles can be performed at much lower temperatures than previously known, the disclosed techniques can offer significant benefit in utilizing waste heat in the production of valuable gaseous fuel.

[0034] As illustrated in FIG. **1**, an exemplary system for preparing a fuel using nanoparticles of an oxygen-storing compound includes a reactor 100, which has an inlet **115** and an outlet **120**. The oxygen-storing compound nanoparticles **105** can be loaded in a support structure **107** at a predetermined position in the reactor, such as a fixed bed of porous inert supports (e.g., porous ceramics) as those commonly used in catalytic reactions or as wash-coats on monoliths as in catalytic convertors of automobiles. The heater **110** can be located in the reactor, e.g., near the support structure **107**, to provide heat of sufficiently high temperature for the reduction of the oxygen-storing compound nanoparticles **105**. Alternatively, the heater **110** can be positioned external to the reactor to preheat a gaseous medium (such as N_2 or O_2) to be introduced into the reactor to contact the oxygen-storing nanoparticles, thereby regulating the temperature of the oxygen-storing nanoparticles. Such an external heater can also be used to preheat CO_2 and/or water vapor to be introduced to the reactor.

[0035] The heater can be coupled with a heat source **160**, which can be waste heat from an industrial process or facility, for example, refinery, chemical plant, nuclear plant or other power plants. The waste heat from these sources can have various grades (i.e. different maximum temperatures). The heat source can also include a solar concentration device or other heat generation devices.

[0036] After the reduction of the oxygen-storing compound nanoparticles **105**, the reduced oxide can be contacted with a gas **125** (CO_2, H_2O or a mixture thereof) introduced from the inlet **115**. The reaction product of the reduced oxygen-storing compound nanoparticles with the gas can include a fuel **130** to be released from outlet **120**.

[0037] The reactions involved in the process can be carried out in a single reaction vessel, and the oxygen-storing nanoparticles need not be moved during the process. However, although shown as a single-vessel structure, the reactor herein can include multiple reaction vessels. The oxygen-storing compound nanoparticles can be loaded in different vessels at different reaction stages. For example, after the initial heating of the oxygen-storing compound nanoparticles in a first vessel at a first temperature, the reduced oxygen-storing nanoparticles can be transferred to a second different vessel to carry out the fuel production reaction at a second temperature. Thereafter, the regenerated oxygen-storing compound nanoparticles can be transferred back to the first vessel for reheating. The second vessel can also be provided with a mechanism to periodically or continuously replace portions of the regenerated oxygen-storing nanoparticles with reduced oxide transferred from the first reactor, thus allowing for

continuous operation of the process. For example, the mechanism can include a supporting structure for accommodating the oxygen-storing nanoparticles, and having an inlet for receiving freshly reduced nanoparticles (e.g., from the first reaction vessel) and an outlet for releasing the "spent nanoparticles" (the nanoparticles after the fuel production reaction has run for a period of time). The inlet and the outlet can be located at opposite ends of the supporting structure. A retrieving device can be used periodically or continuously to remove a portion of the spent nanoparticles from the supporting structure in the second reaction vessel.

[0038] In an alternative embodiment, the support structure can include at least one flow channel having a wall loaded with the oxygen-storing particles. FIG. **9** depicts an example support structure which includes an array of flow channels with the adjacent channels plugged at alternative ends. The walls of the flow channels can be made from a porous material to retain the oxygen-storing particles **105** (e.g., as a wash coat on the channel walls) while allowing a gas to pass through. In this manner, a gaseous medium (e.g., pre-heated by an externally positioned heater) can be introduced into the structure to regulate the temperature of the oxygen-storing nanoparticles. After the oxygen-storing nanoparticles are reduced, CO_2 gas and/or water vapor can be introduced in the structure to produce a fuel at a suitable second temperature, as explained further below.

[0039] For illustration and understanding, the method and system of the disclosed subject matter are described below in conjunction with each other. It is appreciated that the various embodiments of the methods concerning the oxygen-storing nanoparticles and operating conditions are also applicable to the system, and vice versa.

[0040] Using water vapor as an example gas, the reactions occurring during the above described process can be written as:

$$Me_pO_q \longrightarrow Me_pO_{q-y} + y/2\ O_2 \quad (1)$$

$$y\ H_2O + Me_pO_{q-y} \longrightarrow Me_pO_q + y\ H_2 \quad (2)$$

$$y\ H_2O \longrightarrow y/2\ O_2 + y\ H_2 \text{ (net reaction)}$$

where Me_pO_q is the oxygen-storing compound nanoparticles, Me is a metal in the oxygen-storing compound. As will be further described below, Me can include more than one metals. For convenience, the first reaction can be referred to as the nanoparticle-reduction reaction, and the second reaction can be referred to as the fuel-production reaction. The net reaction of the overall process is water vapor being split into oxygen and hydrogen, the latter can be used as a fuel. Using a gas containing CO_2, the second reaction would produce CO and original Me_pO_q. The regenerated Me_pO_q can be reused in reaction (1) and the process can be repeated. As such, although the oxygen-storing compound is involved in the chemical reactions during the process, it is not consumed, and its role in the overall process can be considered catalytic.

[0041] In the above process, the first temperature (or reduction temperature) can be selected to be about 700° C. or lower, 450° C. or lower, or 300° C. or lower. Additionally or alternatively, the heat source can have a temperature of at least 150° C., for example, a temperature of 150-300° C. The second temperature (the gas-nanoparticle reaction temperature) can be same as or different from the first temperature, e.g., from about 200 to about 900° C., from about 250 to about 600° C., from about 300 to 500° C., etc. The second temperature can be selected according to the pressure, purity, or flow speed of the gas fed into the reactor, and the like.

[0042] The oxygen-storing nanoparticles can be, for example, ceria nanoparticles (or nano ceria). As used herein, oxygen-storing nanoparticles, such as nano ceria (or doped nano ceria), can have an average particle size of about 1 to about 100 nm, from 2 to about 50 nm, about 5 to about 20 nm, about 5 to about 15 nm, or from about 5 to about 10 nm. The first reaction where oxygen-storing nanoparticles lose oxygen can also be referred to as the "reduction" of the oxygen-storing nanoparticles. For example, before reduction, nano ceria (CeO_2) can have a small amount of oxygen deficiency (appearing as a few missing oxygen ions, i.e. oxygen vacancies), i.e., in the form of CeO_{2-y} where y is a number from 0 to about 0.06. When ceria is doped, y can increase accordingly. Nano ceria remains in the cubic fluorite crystal-structure without collapsing or changing into a different crystal-structure. After reduction, the oxygen deficiency increases, and y can be a number about 0.5 or smaller, e.g., about 0.15 or smaller. In some embodiments, y can be approximately 0.1. For convenience, "CeO_2" as used herein includes cerium dioxide having some oxygen vacancies.

[0043] Unlike micron-sized or bulk ceria, nano ceria can release oxygen at much lower temperature, e.g., about 800° C. or below. While not wishing to be bound by any particular theory, it is surmised that this property of nano-ceria is due to its increased lattice parameter and a few missing oxygen ions, which results in not only greater oxygen-storage capacity compared with bulk or micro-sized ceria, but lower activation energy for the oxygen to move in and out of the lattice. As shown in FIG. **2**, with decreasing particle size of ceria nanoparticles, the lattice parameter of CeO_2 increases. The increase is particularly pronounced when the particle size is smaller than 20 nm. Compared with micron-sized ceria particles, the increase of lattice parameter of ceria nanoparticles having an average size of about 6 nm is about 0.45%, and with about 1.5% of O^{2-} ions missing (i.e., oxygen vacancies) from the close-packed nature of O^{2-} ions. These seemingly small numbers, however, are significant considering the virtual incompressibility of crystal structure of ceria. The bulk modulus of ceria is reported to be greater than 200 GPa.

[0044] The oxygen-storing nanoparticles, such as nano ceria, can further include one or more dopants, such as a metal or an oxide of the metal, e.g., transition metal such as Cu, Zr, or Pd, or their oxides. Doped oxygen-storing nanoparticles can have increased oxygen-storage capacity, and can also have reduced thermal reduction temperature. In some embodiments, Cu-doped nano ceria where 1-16% (cation-atom ratio), or 5-12% of Ce is replaced by Cu can be used, which can release oxygen at a temperature of below 700° C. In particular, nano Cu—Ceria having about 8% of Cu doping level appear to have high oxygen-storing and release capacity, as is demonstrated in FIG. **3**, which is a H_2-Temperature Program Reduction (TPR) results of Cu—CeO_2 samples having different doping amounts (or loading levels) of Cu (1.6%, 8.2% and 19.6%). In FIG. **3**, the intensity (arbitrary units) signifies the amount of oxygen released from the Cu-doped oxygen-storing nanoparticles at different temperatures as the H_2 is being consumed.

[0045] Other dopants, such as zirconium (e.g., 10-60% of Ce is replaced by Zr) or palladium (e.g., 0.1-5% of Ce is replaced by Pd), can also be used. Other transition metal

dopants, such as Hf, Fe, Co, Cr, Zn, Ni, Ti (or their oxides) can also be used. For example, Hf can be used to replace 0.5-20% Ce in nano ceria. Rare earth metal dopants, such as Y and Gd and their oxides, can also be used, as well as those metals useful as catalysts in the water-gas shift (WGR) reaction, such as Pt, Rh, Au, and Ru or their oxides.

[0046] The dopant can be incorporated into the oxygen-storing nanoparticles by co-precipitation of precursor solutions of a salt of the dopant metal with cerium-containing precursor solutions. For example, methods for preparing Cu-doped nano ceria, Pd-doped nano ceria, and Zr-doped nano ceria, are disclosed in International patent application publications WO2010045484, WO2010062694 and U.S. Pat. No. 6,449,163, the disclosures of all of which are incorporated by reference herein in their entireties. For low levels of doping, e.g., 0.01-5% of transition metal dopant in nano ceria, impregnation of the dopants onto the nano ceria can also be used.

[0047] FIG. **4** depicts the results of a thermogravimetric analysis (TGA) of a sample of Cu-doped nano ceria (29.9 mg, average size ~5 nm) with 8% of Ce replaced by Cu, i.e., $Cu_xCe_{1-x}O_{2-y}$ with x=0.08 (also referred to as 8% Cu—CeO_2 herein. Similarly, r % Me—CeO_2 means that the loading level of the metal Me in CeO_2 is r %). The analysis was conducted in three stages: (1) Heating the sample from room temperature to 700° C. in 100% O_2. The weight loss from room temperature to 300° C. can be from the loss of surface adsorbed gases including water vapor and residual organic or volatile compounds from the synthesis of nano Cu—CeO_2; the weight loss from 450 to 700° C. can be attributed to the reduction of the nano-oxide (i.e., loss of lattice oxygen); (2) Cooling the sample down from 700° C. to 50° C. in 100% O_2: the weight gain can be attributed to re-oxidation of the nano Cu—CeO_2; and (3) Re-heating the sample from 50° C. to 700° C. in 100% N_2. At the end of stage 3 (i.e., as shown by the third curve in FIG. **4**), the weight of the reduced nano Cu—CeO_2 was the same as that of the reduced nano Cu—CeO_2 at the end of stage 1. FIG. **5** is an alternative view of the results of another experiment with the same experimental setup and 8% nano Cu—CeO_2, but a different start sample weight, with time course of the heating-cooling cycle shown on the horizontal axis.

[0048] Approximately 1 wt % loss of nano Cu—CeO_2 (in stage 3) from FIGS. **4** and **5** can be attributed to the reversible loss of lattice oxygen in the Cu—CeO_2 which is thermodynamically prohibited in bulk or micron-size particles of ceria unless the temperature is raised to above 1500° C. or higher. Furthermore, it is noted that the gain of lattice oxygen in stage 2 (cooling in O_2) occurred at very low temperature (below 300° C.), and more significantly, the loss of lattice oxygen in stage 3 (heating in N_2 atmosphere) primarily occurred below 450° C. Most of the oxygen loss occurred below 300° C. This means that in the H_2 or CO production process described above, the temperature for the reduction of nano Cu—CeO_2 can be carried out at a temperature below 700° C., or below 450° C. (or even below 300° C.), depending on the atmosphere in which the nano Cu—CeO_2 is heated. For example, if the nano Cu—CeO_2 is heated in the air, which includes approximately 21% of oxygen, the reduction can occur between 450° C. and 700° C.

[0049] As a comparison with FIG. **4**, FIG. **6** shows a similar heating-cooling-reheating cycle of a pure (i.e., undoped) nano-CeO_2 sample. The oxygen loss at the reheating stage in N_2 also occurs primarily below 450° C. However, the amount of lattice oxygen released from pure nano-CeO_2 is less than one-third of that of the 8% nano Cu—CeO_2. Likewise, FIG. **7** shows a heating-cooling-reheating cycle of a Zr-doped CeO_2 sample ($Zr_{0.38}Ce_{0.62}O_2$). The oxygen loss for this sample at stage 3 is comparable to that of 8% nano Cu—CeO_2 (about 1 wt %).

[0050] The lower temperature and forgiving requirement for the atmosphere for thermal reduction of the oxygen-storing nanoparticles (e.g., ceria or doped nano ceria) can enable the H_2 or CO production process to utilize lower grade heat, such as the exhaust or flue gas produced from industrial process (from power plants, chemical plants, petrochemical plants, etc. that produces waste heat at low temperatures such as 700° C. or lower). Furthermore, conducting the reduction of the oxygen-storing nanoparticles at a lower temperature, such as below 550° C. or below 400° C. can reduce, inhibit, or avoid crystal growth or coarsening at higher temperatures, which negatively impacts the oxygen storage capacity of the material and hinders reuse of the oxygen-storing nanoparticles. As shown in FIG. **8**, a sample of undoped nano ceria of a starting average size of 6.7 nm can coarsen (indicated by the particle-size increase) when heated, and the coarsening is more pronounced when the temperature is greater 550° C. Below 550° C., the coarsening effect is insubstantial. Transition metal doped ceria nanoparticles can have further improved stability against coarsening when heated. For example, below 600° C., nano Zr—CeO_2 can maintain long term particle size stability and oxygen-storing capacity over repeated heating without coarsening.

[0051] FIG. **10** is a diagram depicting an example system for preparing a fuel from a gas using nanoparticles of an oxygen-storing compound according to the disclosed subject matter. As illustrated in FIG. **10**, an exemplary system for preparing a fuel using nanoparticles of an oxygen-storing compound can include a reactor 1000, which has at least one inlet **115** and at least one outlet **120**. The oxygen-storing compound nanoparticles **105** can be loaded in a support structure **107** at a predetermined position in the reactor, as described herein. The heat source **160** can be located in the reactor, e.g., near the support structure **107**, to provide heat of sufficiently high temperature for the reduction of the oxygen-storing compound nanoparticles **105**. Alternatively, the heat source **160** can be positioned external to the reactor to preheat a gaseous medium (such as N_2 or O_2) to be introduced into the reactor to contact the oxygen-storing nanoparticles, thereby regulating the temperature of the oxygen-storing nanoparticles. Such an external heat source **160** can also be used to preheat CO_2 and/or water vapor to be introduced to the reactor. Optionally, the heat source **160** can be coupled with a heater **110**, as described herein.

[0052] The heat source **160** can include any suitable heat source, as described herein. For example, the heat source can include a solar concentration device or other heat generation devices. A solar generation device can receive solar radiation **163**. For example, the solar radiation can be received through a window **161**, which can include a window of any suitable transparent material such as a quartz window **161**. The solar radiation **163** can concentrate the solar radiation using any suitable device. For example, the solar radiation **163** can be concentrated using a compound parabolic collector (CPC) **162**. Additionally or alternatively, suitable devices for concentration of solar radiation can include enclosed troughs, Fresnel reflectors, Dish Stirling, and solar power towers.

[0053] In some embodiments, during the oxygen evolution half-cycle, a purge gas **126** can be introduced from the inlet(s) **115** to reduce oxygen-storing compound nanoparticles **105**. During the fuel production half cycle, the reduced oxide can be contacted with a gas **125** (CO_2, H_2O or a mixture thereof) introduced from the inlet(s) **115**. The reaction product of the reduced oxygen-storing compound nanoparticles with the gas can include a fuel **130** (e.g. H_2, CO, or a mixture thereof) to be released from outlet **120**.

[0054] In some embodiments, the reduction and oxidation of ceria in the presence of carbon dioxide and water vapor can yield carbon monoxide and molecular hydrogen. Mesoporous monolithic ceria can be used to realize such reactions, and the shrinking of particle size and the addition of dopants can reduce the high temperatures required to achieve reduction of carbon dioxide and water vapor. Thremogravimetric analysis (TGA) and a gas chromatography (GC)/mass spectrometry (MS) setup can be used to analyze the reduction of carbon dioxide and water vapor.

[0055] Cerium, classified as a rare-earth metal, can be more abundant than other rare-earth metals. Its abundance in the earth's crust can match that of copper. Cerium can have a density that is greater in the liquid state rather than the solid state. Like water, solid cerium can float in liquid cerium. Cerium (IV) oxide can have the formula CeO_2. Cerium (IV) oxide can exhibits a cubic fluorite lattice structure, space group Fm3m. FIG. **11** is a diagram depicting the lattice structure of cerium (IV) oxide according to some embodiments of the disclosed subject matter. As shown in the figure, cerium **1101** and oxygen **1102** can form the lattice. Additionally, there can be at least one other polymorph, but this other polymorph can exist at extremely high pressures, limiting its relevance.

[0056] A different oxide of cerium, cerium (III) oxide, can be known as cerium sesquioxide. This material can have the formula Ce_2O_3, which can alternatively be represented as $CeO_{1.5}$. FIG. **12** is a diagram depicting the lattice structure of Cerium (III) oxide according to some embodiments of the disclosed subject matter. As shown in the figure, cerium **1101** and oxygen **1102** can form the lattice. The term ceria technically can include all oxides of cerium, including CeO_2, Ce_2O_3, and nonstoichiometric oxides which are typically represented as CeO_2—. The fully reduced Ce_2O_3 can exhibit a hexagonal lattice structure with Pm1 space group symmetry. In some situations, the fully reduced ceria Ce_2O_3 can oxidize to CeO_2 upon exposure to ambient conditions such as air. Alternatively, in certain limited situations (e.g. at very high temperature and low pressure, or in some specially stabilized nanoforms) the cerium sesquioxide can exist in an isolated and pure form. Other forms of ceria (e.g. monoxide and peroxides) can exist under contrived settings.

[0057] Ceria can be applied, for example, in three-way catalytic converters (TWCs). Such devices can be standard in automobiles. TWCs can be relatively complex devices that can incorporate cerium oxide as well as well as aluminum and/or zirconium. In some embodiments, they can be doped with small amounts of platinum, palladium, and/or rhodium. TWCs can catalyze three distinct reactions: the oxidation of carbon monoxide to carbon dioxide, the oxidation of uncombusted small hydrocarbons into carbon dioxide and water, and the reduction of various nitrogen oxides to molecular nitrogen and molecular oxygen. These reactions can act to clean the raw exhaust fumes of an automobile, changing more harmful gasses into less harmful ones.

[0058] Ceria can have high mobility and storage capacity of oxygen within the lattice, and the cerium cations can change oxidation states between +3 and +4 relatively easily. This can be evidenced in the following reaction:

$$CeO_2 \rightarrow CeO_{2-\delta} + \delta/O_2 \quad (1a)$$

[0059] Ceria can be heated to realize reaction (1a). With heat treatment, ceria can reduce and expel oxygen. This can be accomplished in a continuously-refreshing oxygen-free atmosphere to drive the equilibrium of the reaction to the right. If $\delta=0.5$, then the product can be the cerium sesquioxide. In CeO_2, the oxidation state of oxygen can be −2. When molecular oxygen forms, each oxygen atom can leave behind two electrons. These electrons can serve to reduce cerium, which can shift from a +4 oxidation state to a +3 oxidation state. The cubic fluorite structure of ceria can be retained for much of the partial reduction.

[0060] Reaction (1a) can also be expressed in Kröger-Vink notation as follows:

$$O_O^x + 2Ce_{Ce}^x \rightarrow 1/2O_2(g) + V_{O''} + 2Ce'_{Ce} \quad (1b)$$

In this notation, an oxygen and two cerium atoms can occupy their appropriate places in the lattice structure on the reactant side. On the product side, half a unit of molecular oxygen can form, leaving an oxygen vacancy that can have a relative +2 charge. The two cerium atoms can take on a reduced charge, −1 relative to the reactant side.

[0061] Partially reduced ceria can be exposed to molecular oxygen, and the ceria can adsorb the molecular oxygen into its lattice structure. This process can represent the oxidation of ceria, the reverse of reaction (1a). Additionally, partially reduced ceria can oxidize in the presence of alternative oxidants. The oxidation of ceria can bring about the reduction of both carbon dioxide and water, as demonstrated by the following reactions:

$$CeO_{2-\delta} + \delta CO_2 \rightarrow CeO_2 + \delta CO \quad (2a)$$

$$CeO_{2-\delta} + \delta H_2O \rightarrow CeO_2 + \delta H_2 \quad (3a)$$

The reduction of carbon dioxide can yield carbon monoxide and oxidized ceria. The reduction of water can yield molecular hydrogen and oxidized ceria. Reactions (1a), (2a), and (3a) can describe the process fuel production from thermochemical cycles, an exciting developing technology. Additionally or alternatively, other suitable metals can be used, as described herein. Reactions (1a), (2a), and (3a) can be expressed for any suitable metal (M) as follows:

$$1/\delta MO_2 \rightarrow 1/\delta MO_{2-\delta} + 1/2O_2(g) \quad (1c)$$

$$CO_2(g) + 1/\delta MO_{2-\delta} \rightarrow 1/\delta MO_2 + CO(g) \quad (2b)$$

$$H_2O(g) + 1/\delta MO_{2-\delta} \rightarrow 1/\delta MO_2 + H2(g) \quad (3b)$$

[0062] When fossil fuels are burned, carbon dioxide and water can be released.

[0063] The Fischer-Tropsch process can convert molecular hydrogen and carbon monoxide into alkane fuels as shown in the following reaction:

$$(2n+1)H_2 + nCO \rightarrow C_nH_{(2n+2)} + nH_2O \quad (4)$$

This can be a well-understood and efficient process. Both coal and biomass can be used as feedstocks for this process in non-ideal conditions. The metal-oxide thermochemical cycle can eliminate the need for such feedstocks because it can produce the necessary reactants directly from carbon dioxide gas and water vapor.

[0064] The high temperatures used for the reduction of ceria can be achieved by solar means such as the solar generation device heat source **160**. Carbon dioxide can be sequestered from the atmosphere, converted to carbon monoxide through a solar-driven metal-oxide thermochemical cycle, subsequently converted to an alkane liquid fuel via the Fischer-Tropsch process, and combusted to provide energy. The cycle can continue, all driven by the sun. The solar-driven metal-oxide thermochemical cycle can enable such a continuous cycle.

[0065] Referring to FIG. **10**, a device **1000** can use concentrated sunlight to heat a reactor to temperatures in excess of 1500° C. to accomplish reaction (1a). The device can then be allowed to reach a lower temperature, for example, near 900° C., at which point carbon dioxide or water can be introduced to the ceria, yielding reactions (2a) or (3a).

[0066] Catalysis of gas molecules can occur on the surface of metal oxides. In an exemplary embodiment of the devices described herein, the ceria can be mesoporous but monolithic. Particles that are smaller can have a higher ratio of surface area to volume. Carrying out the aforementioned process using ceria nanoparticles (rather than monolithic ceria) can increase the effectiveness of the reaction. Additionally or alternatively, dopants can affect the ceria system. For example, copper, palladium, and/or zirconia dopants can stabilize the ceria so that it can be further reduced and/or resist coarsening effects that could merge the nanoparticles. Either or both of the size reduction of the ceria and the addition of dopants can lower the temperature at which the aforementioned thermochemical cycle can operate, which can increase its commercial viability. For purpose of illustration and not limitation, the reactor temperature can be 900° C. or less, for example, 700-800° C.

[0067] As described herein, the aforementioned devices and/or processes can use any suitable catalyst, including but not limited to the following catalysts. For purpose of illustration and not limitation, commercial micron-sized ceria can be used as a catalyst. This catalyst can behave similarly to mesoporous monolithic ceria, and it can be used as a control. Additionally or alternatively, nanoscale ceria can be used as a catalyst. Nanoscale ceria can show improved catalysis due to its increased surface area. It also can coarsen at temperatures above 500° C. This coarsening can be how larger nanoparticles are accessed. Additionally or alternatively, copper-doped nano ceria can be used as a catalyst. Doping of ceria can increase its oxygen storage capacity or ionic conductivity. For example, 8% copper can be better than greater or lesser amounts of copper in the ceria system. Additionally or alternatively, palladium-doped nano ceria can be used as a catalyst. Additionally or alternatively, zirconia-doped ceria nanoparticles can be used as a catalyst. For example, the addition of zirconia to ceria can stabilize the crystallite size at higher temperatures. For purpose of illustration and not limitation, FIG. **11** illustrates the anti-coarsening effects that zirconia doping can have on ceria nanoparticles. Additionally, for example and not limitation, 50/50 zirconia-ceria can have good thermal stability against coarsening, and such a system can maintain a fluorite structure (at temperatures up to 800° C.) that can facilitate catalysis. Accordingly, $Ce_{0.5}Zr_{0.5}O_2$ nanoparticles can be used as a catalyst, for example.

[0068] In addition to the application of nano ceria catalysts for the solar-driven fuel production using thermochemical cycles, the subject matter disclosed herein can be applied to other technologies. For example and not limitation, the subject matter can be used for hydrogen fuel production. For example, hydrogen fuel can be produced using temperatures in excess of 1000° C. Additionally or alternatively, the subject matter can be adapted to study the water-gas shift reaction (simultaneous oxidation of carbon monoxide and reduction of water).

[0069] Technically, reactions (2a) and (3a) (the reduction of carbon dioxide and water) are not catalyzed reactions because they use up the partially reduced ceria, and, when the ceria is used up, the reaction is over. Strictly speaking, a reagent cannot be a catalyst if it is consumed in a reaction. If reactions (1a) and (2a) are added together, however, the result can be reaction (5), which can represent a catalytic system.

$$CO_2 \xrightarrow{CeO_2} CO + \frac{1}{2} O_2 \quad (5)$$

The steps of the catalytic system can be separated by a thermochemical cycle in which the catalyst is regenerated. Similarly, reactions (1a) and (3a) can be added to yield reaction (6).

$$H_2O \xrightarrow{CeO_2} H_2 + \frac{1}{2} O_2 \quad (6)$$

Reactions (5) and (6) can represent the total systems for carbon monoxide and hydrogen fuel production, respectively.

[0070] Cerium (III) nitrate hexahydrate $Ce(NO_3)_3.6H_2O$ 99.5%, hexamethylenetetramine (HMT) 99+%, copper (III) nitrate demipentahydrate $Cu(NO_3)_3.2.5H_2O$ 98%, palladium (II) nitrate hydrate $Pd(NO_3)_2.xH_2O$ 99+%, and zirconyl chloride octahydrate $ZrOCl_2.8H_2O$ 99% can be commercially available, for example, they can be purchased from Alfa Aesar and used without further purification. Purified water can be prepared to 18 MΩ-cm, for example, with a commercially available Barnstead Nanopure Infinity system.

[0071] Nano ceria can be prepared according to the following exemplary method: 250 mL of aqueous 0.0375 M $Ce(NO_3)_3.6H_2O$ can be prepared and stirred. Separately, and optionally simultaneously, 250 mL of aqueous 0.5 M HMT can be prepared and stirred. After a suitable period of time, for example, thirty minutes, of independent stirring, the solutions can be combined and stirred for a suitable period of time, for example, 16 hours. The solution then can be centrifuged, for example, at 10° C. at 12 krpm for two hours. The supernatant can be discarded, and the solid mass can be left to dry in air, for example, overnight. The solid then can be ground, for example, mechanically ground with a mortar and pestle. This sample can be referred to as nano ceria PR-III-23-A. The aforementioned amounts, time periods, temperatures, and speeds can be adjust by up to −50%, depending on the circumstances.

[0072] Copper-doped nano ceria can be prepared according to the following exemplary method: 200 mL of aqueous 0.040 M $Ce(NO_3)_3.6H_2O$ can be prepared and stirred. Separately, and optionally simultaneously, 200 mL of aqueous 0.5 M HMT can be prepared and stirred. After thirty minutes of independent stirring, the solutions can be combined and stirred for another thirty minutes. 40 mL of 0.0375 M $Cu(NO_3)_3.2.5H_2O$ can be quickly prepared (e.g., within two

minutes +50%) and stirred, and then it can be added to the cerium/HMT solution and stirred for ten minutes. The combined solution then can be added to a water-jacket beaker heated with a circulator bath and allowed to mix for 3 hours at 40° C. The heater then can be turned off and the mixture can be stirred for another eighteen hours. The solution then can be centrifuged at 10° C. at 12 krpm for two hours. The supernatant can be discarded, and the solid mass product can be dried in air at room temperature overnight, after which it can be mechanically ground with a mortar and pestle. This sample can be referred to as 8% Cu-ceria (HS-I-19-A). The percentage can refer to the calculated molar percent of copper cations: $[n_{Cu}/(n_{Cu}+n_{Ce})]*100\%$. ICP studies can be carried out, and they can suggest that the heating of the solution can have no effect. In any case, the ICP studies can indicate an actual copper cation percentage of 7.8%, which can be close to the calculated value based on starting materials. The aforementioned amounts, time periods, temperatures, and speeds can be adjusted by up to ±50%, depending on the circumstances.

[0073] Palladium-doped nano ceria can be prepared according to a similar exemplary method. Three solutions can be independently prepared and stirred for 30 minutes: 200 mL of aqueous 0.0375 M $Ce(NO_3)_3.6H_2O$, 40 mL 0.0042 M $Pd(NO_3)_2.xH_2O$, and 200 mL 0.5 M HMT. After thirty minutes of independent stirring, all three solutions can be combined and stirred for another fifteen minutes. The combined solution then can be added to a water-jacket beaker heated with, for example, a circulator bath and allowed to mix for three hours at 85° C. The heater then can be turned off and the mixture can be stirred for another eighteen hours. The solution then can be centrifuged at 10° C. at 12 krpm for two hours. The supernatant can be discarded. The solid product can be dried in air at room temperature overnight, ground, for example, with a mortar and pestle, and calcined at 400° C. for three hours. This sample can be referred to as 1% Pd-ceria (HS-I-21-B), and the percentage can refer to the calculated molar percent of palladium cations, which can be calculated in the same way as the copper sample. The aforementioned amounts, time periods, temperatures, and speeds can be adjusted by up to ±50%, depending on the circumstances.

[0074] Zirconia-ceria nanoparticles can be prepared based on the method described in commonly assigned International Patent Application No. PCT/US03/03393, the disclosure of which is incorporated herein by reference in its entirety. Separately, and optionally simultaneously, 400 mL of aqueous 0.0375 M $Ce(NO_3)_3.6H_2O$, 400 mL of aqueous 0.0375 M $ZrOCl_2.8H_2O$, and 800 mL of aqueous 0.5 M HMT can be prepared and stirred. After thirty minutes of independent stirring, the solutions can be combined and stirred for 20 hours. The solution then can be centrifuged at 10° C. at 12 krpm for two hours. The supernatant can be discarded. The solid product can be dried in air at room temperature overnight, and then it can be ground, for example, with a mortar and pestle. The powder then can be heated in air. A ramping rate of 100° C./hour for both heating and cooling can be used, and the temperature can be held at a peak of 800° C. for one hour. The sample can be referred to as CZ-50/50 HS-I-23-B. The aforementioned amounts, time periods, temperatures, and speeds can be adjusted by up to +50%, depending on the circumstances.

[0075] Materials can be characterized by x-ray diffraction (XRD), which can be conducted on a commercially available Inel XRG 3000 diffractometer with a curved detector using Cu—K radiation, for example. Data work-up can be done with commercially available MDI JADE software version 2010, for example. These exemplary software packages can use whole-pattern fitting, which can mean that iterations of calculated diffraction patterns can be compared to the experimental pattern until a matching lattice parameter and crystallite size can be reached. The standard reference for lattice parameter can be taken from the Crystallography Open Database (COD ID: 9009008), for example, and the standard reference for large crystallite size can be a scan of the micron-sized Alfa Aesar CeO_2, for example.

TABLE 1

General considerations for TGA

Notebook Reference	Sample	Lattice Parameter (Å)	Particle Diameter (nm)
PR-IV-15-E	Micron ceria	5.41448	>100
PR-III-23-A	Nano ceria	5.43273	9.4
HS-I-19-A	8% Cu-ceria	5.42970	6.1
HS-I-21-B	1% Pd-ceria	5.42683	8.6

[0076] TGA can be the measurement of mass over a range of temperatures. For purpose of illustration and not limitation, TGA studies can be completed on a commercially available Neitzsch STA 449 F3 Jupiter thermogravimetry apparatus. Alumina sample holders can be used throughout. The thermogravimetric chamber can have two scales, one of which can be left with an empty alumina sample holder for internal calibration. The operative scale can be typically loaded with 60-100 mg of material (or left blank for external calibration). There can be a flow of protective nitrogen gas that can enter near the bottom of the chamber and an equal flow of a purge gas that can enter near the top of the chamber. The purge gas can be any suitable gas, for example, either nitrogen or carbon dioxide. Additionally, there can be an additional side gas inlet used for water vapor experiments. For example and not limitation, pure 100% N_2 and pure 100% CO_2 tanks can be used throughout. Additionally, to introduce water vapor, a separate nitrogen line can be bubbled through water at room temperature, allowed to equilibrate, and introduced into the thermogravimetry chamber at appropriate times. Shaded areas of TGA plots can indicate CO_2 or H_2O vapor flow; non-shaded areas can have just N_2 flow. In general, the change of mass in ceria can corresponds to the expelling of molecular oxygen, and the reabsorption of oxygen atoms from either carbon dioxide or water. The possibility of physical adsorption, in addition to the occurrence of the aforementioned chemical reactions, is discussed below.

[0077] Additionally or alternatively, accompanying TEM studies can be undertaken to visually check for any potential changes in crystallite size or morphology. For example and not limitation, dilute suspensions of ceria can be made in ethanol (~2 mg/mL) and drop-cast onto carbon film on 300-mesh copper grid, which can be commercially available from Electron Microscopy Sciences. For purpose of illustration and not limitation, a commercially available JEOLTEM machine can be used to produce TEM images. Measurements of particle diameter can be accomplished, for example, with commercially available Image-J software.

[0078] FIG. **12**A is a diagram depicting an exemplary blank run and FIG. **12**B is a diagram depicting an exemplary run of micron ceria under identical thermogravimetric analysis (TGA) conditions according to some embodiments of the disclosed subject matter. As shown in FIGS. **12**A and **12**B, the

TGA machine can have a tendency to increase mass with increasing temperature and decrease mass with decreasing temperature, even with no sample present. Additionally, as shown in FIGS. **12**A and **12**B, the introduction of carbon dioxide flow can tends to cause a decrease in mass, and the following change back to nitrogen flow can be accompanied by an increase in mass. The aforementioned increase and decrease can be used as baseline considerations. The blank run (FIG. **12**A) and the run with micron ceria (FIG. **12**B) can have similar shape; indeed, when subtracted, the difference can be a flatline for mass. This similarity can indicate that micron ceria can lack redox properties up to 400° C. It can neither reduce to expel oxygen nor oxidize. This can be used as a negative control.

[0079] FIG. **13** is a diagram depicting an exemplary blank TGA run with only N_2 flow according to some embodiments of the disclosed subject matter. Similar to FIGS. **12**A and **12**B, FIG. **13** can show that the TGA machine can have a tendency to increase mass with increasing temperature and decrease mass with decreasing temperature.

[0080] FIGS. **14**A and **14**B are diagrams depicting exemplary runs of calcined 8% Cu—CeO_2 under different TGA experimental conditions according to some embodiments of the disclosed subject matter. For illustration and not limitation, FIG. **14**A can have faster temperature ramp rates, shorter isothermal holding times, and smaller gas flow rates than FIG. **14**B. This can result in the TGA machine failing to keep up with the software-programmed temperatures, and temperatures can fluctuate and fail to be steady at room temperature. The slow gas flow rate can result in the reoxidation of residual CO_2 seen near 400 minutes; residual CO2 can be present due to an incomplete purge of the thermogravimetry chamber atmosphere at low gas flow rates. FIG. **14**A can also indicate that the reoxidation of ceria under CO_2 can occur near room temperature, and can reverse upon mild heating. FIG. **14**B can be produced, with slower temperature ramp rates, longer isothermal holding times, and increased gas flow rates. FIG. **14**B can show desired behavior of ceria: reduction upon heating, staying reduced upon cooling in an inert atmosphere, reoxidation upon exposure to CO_2 oxidant, reaching a flatline equilibrium, and then reducing again with heating in an inert atmosphere. Three reoxidations can be shown with virtually no decrease in catalytic activity.

[0081] FIGS. **15**A and **15**B are diagrams depicting exemplary runs of nano ceria (non-calcined and calcined, respectively) under identical TGA conditions according to some embodiments of the disclosed subject matter. Calcination of the ceria samples can have effects on TGA experiments. FIG. **15**A can show as-made nano ceria exposed to TGA cycles, and FIG. **15**B can show the same TGA run on nano ceria that was previously calcined in air at 400° C. overnight. At least a part of the mass loss depicted in FIG. **15**A can be HMT, water, and other residual surface-adsorbed species. The calcined nano ceria can be introduced to the TGA cycling a short period after cooling down, and the reoxidations can show complete mass uptake back to 100%, which can indicate that the original mass loss in this case can be oxygen expulsion from the lattice. FIGS. **15**A and **15**B both can show mass uptake via reoxidation can represent about a 2% increase, and this result can be more clear in FIG. **15**B. The difference in peak heights for FIG. **15**B can be ascribed to TGA cycle design; other experiments can show a consistent peak height. Also, upon prolonged exposure to ambient conditions and air, calcined ceria can re-adsorb water vapor on its surface. This can explain the different in relative peak heights in FIGS. **14**A and **14**B FIG. **3**: FIG. **14**A can depict a sample that had been very recently calcined, while FIG. **14**B can depict a sample that had been previously calcined but exposed to ambient conditions for several days. In either case, the re-oxidation mass uptake can be about 2%. This calcination effect can negatively impact clarity. Other experiments can show that flowing dry inert gas over the sample in the TGA before starting data collection can remove surface-adsorbed species. Even in samples that have been exposed to ambient conditions for several days, this pre-flow can cause the subsequent reoxidations to return a 100% mass.

[0082] The surface-adsorbed species can be not visible by TEM or XRD. For purpose of illustration and not limitation, a series of experiments can test the size and morphology of ceria samples before and after overnight 400° C. calcination, and these experiments can find virtually no difference between the two groups. For example and not limitation, TEM studies on commercially available micron CeO_2 (e.g., Cerium (IV) oxide CeO_2 99.99% from Alfa Aesar, advertised as 14 micron powder) can confirm that such ceria can have a crystallite size that can be in excess of 100 nm, with heat annealing at 400° C. having no significant effect on particle size or morphology. FIG. **16** is a TEM image of an exemplary unheated commercial micron ceria sample. For micron ceria, TGA can appear similar or identical before and after heat annealing, indicating that the micron ceria can tend not to adsorb on its surface.

[0083] FIG. **17**A is an exemplary TEM image of PR-IV-23-A ceria, made with hexamethylenetetramine (HMT) and no heat annealing. A particle diameter of 9.4 nm can be determined by XRD, and a particle diameter of 8.4 nm can be determined by cursory TEM inspection. FIG. **17**B is an exemplary TEM image of the same sample treated at 400° C. overnight (PR-IV-35-C ceria). A particle diameter of 9.0 nm can be determined by XRD, and a particle diameter of 9.1 nm can be determined by TEM. FIGS. **17**A and **17**B can study the effects of heat annealing at 400° C. on un-doped nano ceria. Polydispersity in both cases can be minimal. As shown by comparing FIGS. **17**A and **17**B, the effects of heat annealing can be negligible when measured by XRD and TEM. However, the effects can be large when measured by TGA, as can be seen in FIGS. **15**A and **15**B.

[0084] FIG. **18**A is an exemplary TEM image of an exemplary 8% Cu-ceria sample (HS-I-19-A) that has not been heat annealed, and FIG. **18**B is an exemplary TEM image of the same sample after being heat annealed at 400° C. overnight (PR-IV-34-A). Referring to FIG. **18**A, a particle diameter of 6.1 nm can be determined by XRD, and a particle diameter of 6.3 nm can be determined by TEM, and the nanoparticles can demonstrate monodispersity such that they can be about the same size. Referring to FIG. **18**B, a particle diameter of 6.5 nm can be determined by XRD, and a particle diameter of roughly 5.7 nm can be determined by TEM, with good monodispersity. FIGS. **18**A and **18**B can display effect of heat annealing at 400° C. on 8% Cu-ceria, effects which can be insignificant when measured by XRD and TEM.

[0085] FIGS. **19**A, **19**B, and **19**C are diagrams depicting exemplary CO_2 TGA runs of nano ceria, copper-doped ceria, and palladium-doped ceria, respectively. These Figures can show TGA cycles for each of these three ceria systems. All three of these Figures can show loss of mass during heating and significant increase of mass upon exposure to CO_2. The can also show virtually no decrease in catalytic activity over

three cycles. The mass uptakes per cycle can be similar, but copper-doped ceria can appear to have a slight advantage at about 2.5% mass uptake with CO_2 exposure, followed by nano ceria at about 2.0%, and palladium-doped ceria at about 1.5%. Each of these systems can cycle between 400° C. and 25° C., which can be an improvement over certain systems with cycling temperatures between 1500° C. and 900° C. The advantage realized by the copper-doped system can be amplified at slightly higher temperatures.

[0086] FIG. **20** is a diagram depicting an exemplary TGA run of copper-doped ceria. Catalytic activity for copper-doped ceria can cease when heating temperatures reach 800° C. or more. The ceria can reduce fairly continuously up to 800° C., and upon subsequent exposure to CO_2 at room temperature, no mass uptake can be recorded. The mass change upon exposure to CO_2 in this case can match with the baseline changes seen in blank samples (e.g., as described herein regarding FIGS. **12**A and **12**B).

[0087] FIG. **21** is an exemplary TEM image of copper-doped ceria after TGA cycling up to 800° C. (PR-IV-41-A). TEM imaging can confirm the coarsening of the copper-doped ceria exposed to 800° C. TGA cycling. This coarsening can explain the loss in catalytic activity. For example and not limitation, the lack of catalytic activity can be consistent with the increased particle size seen in FIG. **21**. Copper apparently can be ineffective at protecting against coarsening at 800° C.

[0088] FIGS. **22**A and **22**B are diagrams depicting exemplary TGA runs of zirconia-doped ceria. As described herein, zirconia dopants can prevent coarsening of ceria nanoparticles. Certain zirconia-ceria nanoparticles can show no catalytic activity at either 600° C. or 400° C. As shown in FIGS. **22**A and **22**B, no mass uptake can be observed upon exposure to CO_2.

[0089] FIG. **23** is an exemplary TEM image of 50/50 zirconia-ceria nanoparticles synthesized including an 800° C. calcination step. TEM imaging of zirconia-ceria can confirm lack of nanoparticle coarsening after exposure to 800° C.

[0090] FIGS. **24**A and **24**B are diagrams depicting exemplary runs of N_2/H_2O TGA cycling up to 400° C. with blank (FIG. **24**A) and micron CeO_2 (FIG. **24**B). Shaded areas can indicate flow of N_2 saturated with H_2O, non-shaded areas can indicate N_2 flow. FIGS. **24**A and **24**B can be used as blank and negative control TGA cycles, respectively. A trend of small positive correlations between heating and mass increase (or cooling and mass decrease) can be observed. Additionally, a small increase in mass can be seen upon introduction of water vapor. The blank and micron ceria runs can have similar shape. When the latter is subtracted from the former, the product can be a flat mass baseline, which can indicate that micron ceria can show no redox properties under these conditions. The saturation of water vapor pressure at room temperature can be about 2%.

[0091] TGA cycling of nanoparticles with water vapor can indicate that the reoxidation of ceria with water can be enhanced at room temperature (much like reoxidation with carbon dioxide). Raising the temperature under a water vapor atmosphere can result in reversible weight loss similar to FIG. **14**A.

[0092] FIGS. **25**A, **25**B, and **25**C are diagrams depicting exemplary H_2O TGA runs of nano ceria, copper-doped ceria, and palladium-doped ceria, respectively. The TGA cycles can be calibrated for water vapor flow as described herein regarding the CO_2 cycles. As shown in these Figures, the mass can increase beyond 100% after exposure to water vapor. At least part of this mass increase can represent oxygen incorporation into the lattice and a correspondingly large amount of hydrogen gas production. Additionally or alternatively, the mass increase can be due to the adsorption of water molecules onto the surface of the nanoparticles. Additionally, both processes can occur. Additionally, passing dry nitrogen over samples can remove adsorbed water. In FIGS. **25**B and **25**C, the mass can decrease upon exposure to dry N_2 gas, level off, and then decrease further upon heating. This can indicate that the first decrease can be due to the removal of adsorbed water, while the second decrease can be due to the reduction of ceria and expulsion of lattice oxygen. FIGS. **25**A, **25**B, and **25**C can indicate that the ceria nanoparticles can behave as desired and reduce H_2O to H_2 with temperature cycling up to 400° C. As in the CO_2 cases described herein, there can be evidence for an advantage to copper or palladium dopants.

[0093] FIG. **26** is an exemplary TEM image of 8% Cu-ceria after N_2/H_2O TGA treatment (PR-IV-34-A). No visible change to nanoparticles subject to 400° C. H_2O cycles can be observed.

[0094] To further confirm the proposed reduction and oxidation reactions, the following gaseous products can be directly detected: carbon monoxide and hydrogen. Oxygen also can be detected during heating steps. For purpose of illustration and not limitation, for direct detection studies, the TGA gas outlet can be connected to either a micro gas chromatography (GC) unit and/or mass spectrometry (MS) set up such as a commercially available Agilent 5973 Network Mass Selective Detector Spectrometer. The GC can have moderate sensitivity and can sample the gas flow every two minutes. The MS can have good sensitivity and can sample the gas flow on a sub-second frequency.

[0095] For example and not limitation, TGA runs (similar to FIGS. **19**A, **19**B, **19**C, **25**A, **25**B, and **25**C) can be set up with GC and MS monitoring of the outlet of the TGA chamber. The GC can detect nitrogen, oxygen, carbon dioxide, carbon monoxide, and hydrogen. The GC can be unable to detect water. For the water TGA cycling, nitrogen can be detected throughout the TGA run. Oxygen and hydrogen can be undetected. For the carbon dioxide TGA cycling, nitrogen can be detected throughout, and carbon dioxide can be detected at the expected time. Oxygen and carbon monoxide can be undetected.

[0096] For purpose of illustration and not limitation, TGA runs can be set up with MS monitoring. Carbon monoxide and nitrogen can have the same mass, so helium can be used as the inert gas. Helium can be a poor purge gas (which can be due to its low mass). Additionally or alternatively, argon can be used as the inert gas. MS measurements can be problematic because carbon dioxide can degrade to carbon monoxide during the spectrometry process, so even a stream of pure carbon dioxide will show carbon monoxide detection. Additionally, very light gasses can sometimes not be detected by MS. For example, a 0.1% hydrogen in nitrogen mixture can be detected as nitrogen. As another example, with a flow mixture of 50% helium in carbon dioxide, only the carbon dioxide can be detected by MS, although the MS will detect the helium after a thorough purge with pure helium. TGA cycling with carbon dioxide can show disappointing results: no oxygen can be observed upon heating, and no excess carbon monoxide can be observed upon exposure to carbon dioxide, both in helium and argon carrier gas.

[0097] FIG. **27** is a diagram depicting exemplary TGA cycling between 150° C. and 450° C. For purpose of illustra-

tion and not limitation, a copper-doped ceria sample can be heated from room temperature to 150° C. At this temperature, it can be unlikely that there are physical adsorbents on the ceria. For example, water can be completely vaporized at this temperature. After holding the sample at 150° C., the sample can be further heated to 450° C. If physical absorbents were solely responsible for the mass changes, then there should be no change in mass between 150° C. and 450° C. Instead, the mass of ceria further decreases with this further heating. This further decrease can indicate that the mass change can be due at least in part to the further reduction of ceria and expulsion of lattice oxygen. The ceria then can be reoxidized upon exposure to carbon dioxide at 150° C. MS detection of the TGA cycle depicted in FIG. **27** can show only argon and carbon dioxide. Additionally or alternatively, physical adsorption of CO_2 is possible in different materials in temperatures up to 260° C.

[0098] For purpose of illustration and not limitation, GC and MS monitoring can fail to detect O_2, CO, and/or H_2 due to a gas flow mixing issue or a concentration issue in the TGA. For example, a separate experiment can be set up with a reactor chamber and 1500 mg of copper-doped nano ceria. The ceria can be heated up and cooled in an argon atmosphere, then the reaction chamber can be sealed. Carbon dioxide can be introduced with a syringe, and then the gas in the chamber cab be analyzed by GC. The quantities and volumes can be well beyond the detection limit of the GC. The GC can fail to detect CO.

[0099] Direct detection of ceria thermocycling products can be achieved using furnaces, MS, and GC. Sample sizes can range from 250-1000 mg, which can be greater than the 100 mg sample sizes considered herein but less than the 1500 mg sample of copper-doped nano ceria considered herein. MS can be used for the detection of hydrogen, and GC can be used for the detection of carbon monoxide. Additionally, sampling of an outlet gas stream can be problematic for gas detection, for example, because MS can be designed for direct injection of a sample. MS detection can prefer high mass gasses. The preference can be due to gas mixing in the thermogravimetry chamber, gas flow through the tubing system, gas intake at the MS inlet, or the MS itself. Detection of small masses can be enhanced with direct injection, which can bypass the potential gas mixing concerns.

[0100] Direct detection of gasses can be achieved on a larger scale. For example and not limitation, several grams of ceria catalyst can be synthesized and tested in a packed-bed reactor. The sample can be heated and cooled in inert gas, then sealed. A small amount of oxidant gas can be injected into the sealed chamber. The gas sample can be allowed to react, then can be directly injected into a GC/MS setup to detect the desired product, for example, hydrogen or carbon dioxide. This process can solve the problem of direct detection and support the results obtained based on TGA data.

[0101] The TGA cycles discussed herein can demonstrate that nano ceria interacts with oxidant gases differently than micron ceria. This result can agree with the observation that the surface of nano ceria can be different from the surface of micron ceria. It can be possible, with slight changes in temperatures, materials, and reactor conditions, which the solar-driven thermochemical fuel cycle can work at lower temperatures.

[0102] The foregoing merely illustrates the principles of the disclosed subject matter. Various modifications and alterations to the described embodiments will be apparent to those skilled in the art in view of the disclosure herein. It will thus be appreciated that those skilled in the art will be able to devise numerous methods which, although not explicitly shown or described herein, embody the principles of the disclosed subject matter and are thus within its spirit and scope of the appended claims.

1. A method for preparing a fuel from an oxygen-storing compound in the form of nanoparticles, comprising:

heating the nanoparticles at a first temperature to release an amount of oxygen, thereby producing a reduced oxide compound; and

exposing the reduced oxide compound to a gas at a second temperature to produce the fuel, wherein the gas is selected from the group consisting of carbon dioxide and water vapor.

2. The method of claim **1**, further comprising selecting the second temperature to be less than the first temperature.

3. The method of claim **1**, further comprising selecting the first temperature to be about 700° C. or lower.

4. The method of claim **1**, further comprising selecting the first temperature to be about 450° C. or lower.

5. The method of claim **1**, further comprising selecting the first temperature to be about 150° C. to about 300° C.

6. The method of claim **1**, wherein the fuel comprises at least one of carbon monoxide and molecular hydrogen.

7. The method of claim **1**, wherein the oxygen-storing compound comprises cerium oxide.

8. The method of claim **1**, wherein the oxygen-storing compound comprises cerium oxide doped with a transition metal or an oxide thereof.

9. The method of claim **1**, wherein the oxygen-storing compound comprises a cerium oxide doped with a rare earth metal or an oxide thereof.

10. The method of claim **8**, wherein the transition metal comprises a metal selected from the group consisting of Cu, Zr, and Pd.

11. The method of claim **8**, wherein the transition metal comprises a metal selected from the group consisting of Hf, Fe, Co, Cr, Zn, Ni, Au, Ti, Pt, Rh, and Ru.

12. The method of claim **10**, wherein the transition metal comprises Cu such that Cu replaces about 5% to about 10% of cerium in the cerium oxide.

13. The method of claim **12**, wherein the Cu replaces about 8% of cerium in the cerium oxide.

14. The method of claim **1**, wherein the average size of the nanoparticles of the oxygen-storing compound is about 2 to about 15 nm.

15. A system for preparing a fuel using nanoparticles of an oxygen-storing compound and a gas selected from the group consisting of carbon dioxide and water vapor, comprising:

a reactor adapted to receive nanoparticles of the oxygen-storing compound in a predetermined location therein and the gas through a gas intake;

a heater adapted to heat the oxygen-storing nanoparticles to a first temperature to reduce the nanoparticles to form a reduced oxygen-storing compound;

wherein the gas intake is positioned to deliver the gas to contact the reduced oxygen-storing compound at a second temperature, thereby converting at least a portion of the gas to the fuel.

16. The system of claim **15**, wherein the fuel comprises at least one of carbon monoxide and molecular hydrogen.

17. The system of claim **15**, wherein the heater is configured to deliver heat having a maximum temperature of about 450° C.

18. The system of claim **17**, wherein the heater is coupled with a heat source having a maximum temperature of about 450° C. or lower.

19. The system of claim **17**, wherein the heat source is waste heat from an industrial process.

20. The system of claim **17**, wherein the heater is coupled with a solar concentration device.

21. The system of claim **15**, wherein the oxygen-storing compound comprises cerium oxide.

22. The system of claim **15**, wherein the oxygen-storing compound comprises cerium oxide doped with a transition metal or an oxide thereof.

23. The system of claim **21**, wherein the transition metal comprises a metal selected from the group consisting of Cu, Zr, and Pd.

24. The system of claim **15**, wherein the average size of the nanoparticles of the oxygen-storing compound is about 2 to about 15 nm.

25. The system of claim **15**, further comprising a support structure having at least one flow channel having a gas-permeable wall, the oxygen-storing nanoparticles loaded on the support structure.

* * * * *